A Review of Solar Methane Reforming Systems

Elysia J. Sheu[a], Esmail M. A. Mokheimer[b], Ahmed F. Ghoniem[a,*]

[a]*Department of Mechanical Engineering, Massachusetts Institute of Technology, 77 Massachusetts Avenue, Cambridge, MA, USA*
[b]*Department of Mechanical Engineering, King Fahd University of Petroleum and Minerals, Dhahran 31261, Saudi Arabia*

Abstract

Because of the increasing demand for energy and the associated rise in greenhouse gas emissions, there is much interest in the use of renewable sources such as solar energy in electricity and fuels generation. One problem with solar energy, however, is that it is difficult to economically convert the radiation into usable energy at the desired locations and times, both daily and seasonally. One method to overcome this space-time intermittency is through the production of chemical fuels. In particular, solar reforming is a promising method for producing chemical fuels by reforming and/or water/carbon dioxide splitting. In this paper, a review of solar reforming systems is presented, as well as a comparison between these systems and a discussion on areas for potential innovation including chemical looping and membrane reactors. Moreover, a brief overview of catalysis in the context of reforming is presented.

Keywords: Hybrid Solar-Fossil Fuel, Solar Reforming, Fuel Conversion, Solar receiver-reactor

*Corresponding Author: ghoniem@mit.edu, Tel: +1 6172532295, Fax: +1 6172535981

Nomenclature

Latin Letters

ΔH^o	Standard Enthalpy of Reaction	kJ/mol
Q	Heat Input	W
$\dot{n}$	Molar Flow Rate	mol/s

Greek Letters

η	Efficiency or Conversion

Subscripts

$solar$	Solar Input
$fuel$	Fuel Input
$conv$	fuel conversion
$chem$	Chemical

1. Introduction

As the world's population, standards of living, and economy continue to grow, energy demand rises significantly, leading to higher emissions, especially in greenhouse gases. Much work has been done to expand the use of renewable energy sources (such as solar energy) to meet these demands while curtailing emissions. Solar energy has the potential to provide all the world's

energy demands; however, converting solar radiation into useful energy forms at the desired times and locations and at a reasonable cost is challenging.

One method of converting solar radiation into usable energy is the production of chemical fuels. This, in essence, creates a means of relatively easy storage and transportation of the solar energy [1, 2, 3]. This conversion can be achieved through a number of different ways including (i) thermochemical cycles for splitting water and carbon dioxide, (ii) solar cracking/gasification of solid fuels, and (iii) solar reforming of liquid and gaseous hydrocarbons [4, 5, 6, 7]. Thermochemical cycles for water splitting involve using heat sources to dissociate water into hydrogen and oxygen. While most desirable, water splitting requires very high temperatures outside most solar collection technologies [8]. The temperature can potentially be lowered through the use of membranes to remove oxygen or hydrogen and shift the equilibrium towards further dissociation [9] or chemical looping processes using oxygen carriers [10, 11, 12]. Solar cracking involves using heat to decompose a hydrocarbon into hydrogen and carbon, and similar to water splitting, temperatures required for methane decomposition can also be very high unless a separation process is used [8, 13]. Solar reforming, on the other hand, can achieve significant conversion at relatively lower temperatures using catalysts to speed up the kinetics. Therefore, even though some CO_2 emissions are produced when using hydrocarbons, solar reforming is considered a promising method for converting solar radiation into chemical fuels [8, 14], and hence is the focus of this review. It should be noted that in some reforming concepts such as chemical looping, the reforming system actually blurs the line between the different methods of converting solar radiation into chemical

fuels, and the system can involve more than one method of conversion (i.e., reforming and water splitting). Therefore even though these systems are not strictly reforming systems, they will also be discussed.

Solar reforming is similar to traditional reforming except the solar energy is used to provide the high temperature heat source rather than burning extra fuel (or using nuclear heat). In most cases, a hydrocarbon fuel, such as natural gas, is reformed into syngas (a mixture of H_2 and CO) which has a higher heating value. With the additional step of water-gas shift, pure hydrogen can be produced after separating CO_2. A solar reforming system typically consists of two main parts: (i) a solar collector/concentrator and (ii) a chemical reactor [15]. The solar collector is (a) a trough, (b) a central receiver tower, or (c) a parabolic dish. The solar collector is used to raise the temperature of a heat transfer fluid that is used within the chemical reactor, or to directly heat the chemical reactor. The chemical reactor, of course, is where the catalyst-assisted reforming reactions occur.

The most common reforming processes used in solar systems are steam or CO_2 (dry) reforming. The key reactions for the two processes (steam and dry reforming, respectively) are shown below for the case of methane [16]:

$$\mathrm{CH_4 + H_2O}(v) \xleftrightarrow{energy} \mathrm{CO + 3H_2} \quad \Delta H^o = 205\mathrm{kJ/mol} \tag{1}$$

$$\mathrm{CH_4 + H_2O}(l) \xleftrightarrow{energy} \mathrm{CO + 3H_2} \quad \Delta H^o = 250\mathrm{kJ/mol} \tag{2}$$

$$\mathrm{CH_4 + CO_2} \xleftrightarrow{energy} \mathrm{2CO + 2H_2} \quad \Delta H^o = 246\mathrm{kJ/mol} \tag{3}$$

The enthalpy of reaction for steam reforming is approximately 23% of the enthalpy of combustion of methane, and hence the heating value of the syngas

is 25% higher by the same amount. Water vapor is typically used in the steam reforming reactions rather than liquid water. The enthalpy of reaction for dry reforming is approximately 28% of the enthalpy of combustion of methane, and the heating value of the syngas can be as much as 30% higher than the input methane.

Most often, the water-gas shift reaction occurs in conjunction with the reforming reactions. The water gas shift reaction is shown below [16]:

$$\mathrm{CO} + \mathrm{H_2O} \xleftrightarrow{energy} \mathrm{CO_2} + \mathrm{H_2} \quad \Delta H = -41\mathrm{kJ/mol} \tag{4}$$

For steam reforming, a steam methane ratio of 2:1 to 3:1 is required in order to obtain full conversion at reasonable temperatures, and to prevent coke formation (i.e., the thermal cracking of hydrocarbon occurring in parallel with steam reforming) [17]. With dry reforming, the process typically runs at a 1:1 ratio. Methane conversion (at equilibrium) for various temperatures and pressures for the two reactions is shown in Figures 1 and 2, with steam to methane ratio of 3, and carbon dioxide to methane ratio of 1. For reference, the combined steam reforming and water-gas shift stoichiometric reaction for a 3:1 steam to methane ratio is shown below:

$$\mathrm{CH_4} + 3\mathrm{H_2O} \xrightarrow{energy} \frac{7}{2}\mathrm{H_2} + \frac{1}{2}\mathrm{CO} + \frac{1}{2}\mathrm{CO_2} + \frac{3}{2}\mathrm{H_2O} \tag{5}$$

All equilibrium calculations are performed with an equilibrium reactor model (which calculates the outlet composition based on minimizing the Gibbs free energy) in Aspen Plus, and the water-gas shift reaction is considered in the calculations.

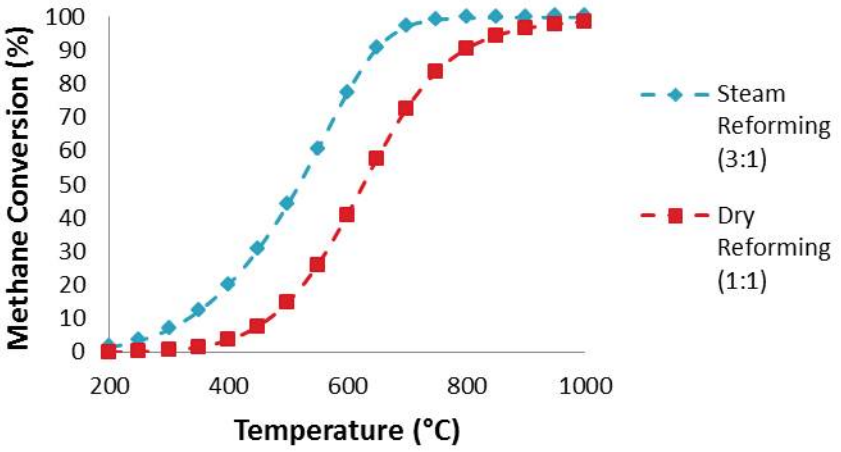

Figure 1: Temperature dependence of methane conversion at equilibrium for steam and dry reforming (Pressure = 1 atm)

From Figure 1, it can be seen that higher temperatures are preferred for methane conversion, given that both reactions are highly endothermic. Steam reforming for the 3:1 ratio reaches full conversion at lower temperatures than dry reforming due to the higher enthalpy of reaction of the latter (and the higher steam to methane ratio). From Figure 2, it can be seen that lower pressures are preferred for methane conversion, as volume expansion occurs during the process [17]. The reforming process has a much greater dependence on temperature than pressure.

Syngas produced from reforming processes can be used as a fuel in a gas turbine or a solid oxide fuel cell, or the hydrogen generated by shifting the CO in low a temperature fuel cell [18]. If CO_2 produced during reforming is captured, syngas combustion would lead to a reduction in CO_2 emissions of as high as 22% when compared to combustion of methane [19]. Some preliminary cost analysis of these solar reformers (dry reforming of methane)

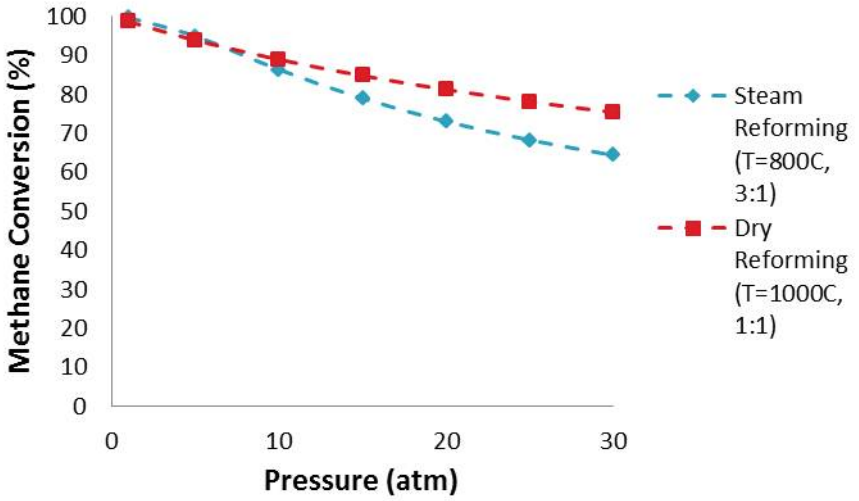

Figure 2: Pressure dependence of methane conversion at equilibrium for steam and dry reforming

has been done [20, 21]. The cost was analyzed for a 50 MW_{th} solar reforming plant, and it was found that the cost of producing hydrogen was approximately 20% higher for the solar reforming system when compared to traditional reforming systems [20, 21]. The higher cost is due to the additional expenses associated with solar collectors and concentrators. However, if subsidies are included, solar reforming could be favorable [20, 21].

The performance of the reforming system can be evaluated using a number of metrics. In this review, reforming systems will be evaluated on the basis of (if given) (i) chemical efficiency, (ii) fuel conversion, (iii) catalytic activity and stability, and (iv) residence time. Chemical efficiency is defined as the percent of solar energy transferred to the solar reforming product (syngas -

CO and H_2) as chemical enthalpy change,

$$\eta_{chem} = \frac{\dot{n}_{prod}\Delta H_{prod}}{\dot{Q}_{solar}} \tag{6}$$

where η_{chem} is the chemical efficiency, $\dot{n}_{prod}$ is the product molar flow rate, ΔH_{prod} is the chemical enthalpy change of the products with respect to the reactants, and Q_{solar} is the solar energy input. Fuel conversion is defined as the percentage of input fuel (usually methane) converted into the reforming product (usually syngas) - essentially anything that is not part of the original fuel. The methane conversion in equation form is defined as

$$X = 1 - \frac{\dot{n}_{fuel,out}}{\dot{n}_{fuel,in}} \tag{7}$$

where X is the methane conversion, $\dot{n}_{fuel,out}$ is the molar flow rate of fuel in the reformer product, and $\dot{n}_{fuel,in}$ is the molar flow rate of fuel flowing into the reformer. The outlet composition of the reformer can contain the input fuel since fuel conversion will most likely never be 100%.

The reactor performance can be affected by a number of different design aspects including what catalyst is used/ how it is prepared, how the reactor is heated/absorbs the solar radiation, how the gases come in contact with the catalyst (mass transfer effects). These different design aspects can affect the methane conversion/chemical efficiency but also the temperature distribution within the reactor. The temperature distribution/variation within the reactor is important as large temperature variations can lead to large thermal stresses, which in turn, can be detrimental to the solar reformer's long term operation stability. The discussion of current solar reformers will

include these different aspects and their impact on performance.

This review organizes the different systems based on reforming process. Within each category the reformer is classified as either a directly heated or an indirectly heated system. While previous work classified direct and indirect systems based on whether the fluid or particles come in direct contact with the solar radiation [22, 23], in this review, directly heated denotes systems where the solar receiver and reactor are one integrated unit and thus the reactor is directly heated by the solar energy. Indirectly heated systems are those in which the solar receiver and reactor are two separate units and the solar energy is used to heat some intermediary heat transfer fluid which in turn is used to heat up the reactor. In the remaining parts of the paper, a brief discussion of catalysis as it relates to reforming is presented. Next, work on these solar reforming systems is discussed, followed by a comparison of these different types of reforming systems. Potential areas for innovation are presented, followed by concluding remarks.

2. Reforming Catalysis

Before examining progress on various solar reforming reactor systems (defined as reforming reactor plus the solar concentrator/collector), a brief discussion on reforming catalysis is presented. A more in depth review and discussion of catalysts for solar reforming can be found in [24].

As shown previously, in reforming processes such as steam and dry reforming of methane, there are thermodynamic limitations for how much conversion can be achieved at a given temperature and pressure. These equilibrium limits are calculated based on the assumption of infinite time (i.e., how long

it takes for the reforming process to achieve this thermodynamic limit is not accounted for). Reforming reactors are of finite size and hence more likely to be kinetically limited by the available residence time. Thus, to achieve significant fuel conversion at reasonable flow rates, catalysts are often used to speed up the reactions. Reforming catalysts typically consist of an active metal dispersed on a ceramic support. The catalytic surface provides an alternative route for the chemical reactions that is more energetically favored than the gas phase reactions, which in turn "speeds up" the reforming reactions and allows for fuel conversion at reasonable rates [25]. A schematic of the energetics for a catalyzed versus non-catalyzed reaction is shown in Figure 3. Essentially the catalyst decreases the activation energy required for the reaction to proceed thus speeding up the conversion.

A catalyst has three main components: (1) the active metal, (2) a promoter, and (3) the ceramic support. For reforming, the active metal is usually either a transition group metal (i.e., Ni, Fe, or Co) or a noble metal (i.e., Ru, Rh, Ir, Pt, or Pd) [26, 27, 28, 29, 30]. There has also been studies on bimetallic catalysts and transition metal carbide catalysts [26, 31, 32, 33]. Promoters most often used in reforming catalysts include alkaline earth metals such as Mg or Ca, rare earth metals such as Ce or La, and transition metals like Zr [34, 35]. The most common ceramic support used for reforming catalysts is Alumina, but there have also been studies investigating other types of supports including SiO_2, ZrO_2, TiO_2, La_2O_3, and CeO_2 [26, 34].

Since there are many choices for the catalyst design, a number of issues must be considered, including cost, activity, and durability. These characteristics depend not only on the metal/promoter/support chosen but also

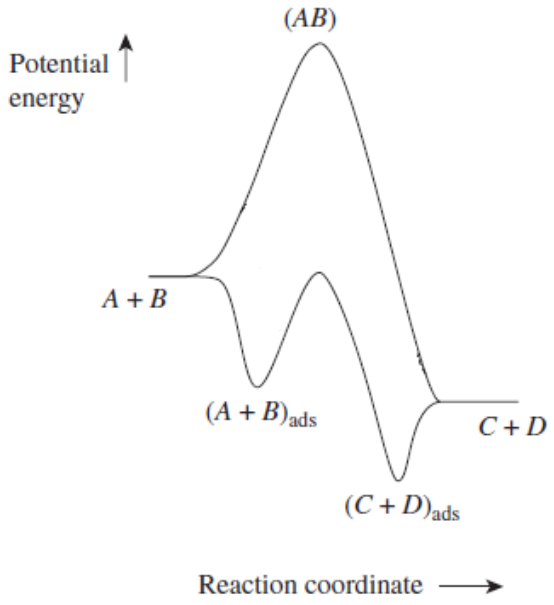

Figure 3: Schematic of energetics for catalyzed and non-catalyzed reaction A+B →C+D: $(A+B)_{ads}$ and $(C+D)_{ads}$ represent catalyzed reaction and (AB) represents non-catalyzed reaction [25]

on the type of reformer. As will be discussed in more detail later, directly heated reformer systems can reach higher temperatures which enables higher fuel conversion. However, these higher temperatures can also cause catalyst sintering and lower its activity and durability. In addition, higher operating temperatures can lead to carbon deposition which degrades the catalyst and affects its activity and durability. A comparison, based on these three aspects, of the most commonly used reforming catalysts will now be discussed.

In terms of the activity, there have been different rankings reported in the literature. Some studies suggest that the activity ranking is as follows

[28, 36, 37]:

$$\text{Ru} \approx \text{Rh} > \text{Ni} \approx \text{Pd} \approx \text{Pt} > \text{Co} \quad \text{(Steam Reforming)} \tag{8}$$

$$\text{Ru} \approx \text{Rh} > \text{Ir} > \text{Ni} > \text{Pt} \approx \text{Pd} \quad \text{(Dry Reforming)} \tag{9}$$

Other studies have suggested the following ranking for both steam and dry reforming [38, 39]:

$$\text{Pt} > \text{Ir} > \text{Rh} > \text{Ru} \approx \text{Ni} \tag{10}$$

Regardless of the exact order of the metals themselves, most studies show that, in general, noble metals have at least the same or even higher activity than transition metals like Ni or Co. The activity affects the amount of active metal needed. Typical loading for noble metal catalysts are in the range of 0.2 - 5 wt% which is much lower than typical loading used for transition metal catalysts like Ni (10-15 wt%) due to this higher activity.

When accounting for catalyst durability, the temperature at which the catalyst starts to degrade or sinter, as well as the temperature at which carbon deposition on the catalyst starts must be considered. Transition metal catalysts like Ni experience sintering at typical operating temperatures of solar reformers. In addition, Ni catalysts promote carbon deposition, which limits the reforming conditions for which a Ni catalyst can be used. For instance, in steam reforming using a Ni catalyst, steam to fuel ratio of approximately 3 are required in order to avoid carbon deposition [17]. The susceptibility of transition metal catalysts like Ni to sintering and carbon deposition can be reduced by using an appropriate support [26]. Noble metals on the other hand, are much more stable against carbon deposition and also

sinter at much higher temperatures [40, 28, 30].

For catalyst cost, noble metals cost more than transition metals (Figure 4). From Figure 4 it can be seen that among noble metals, Ru is the cheapest,

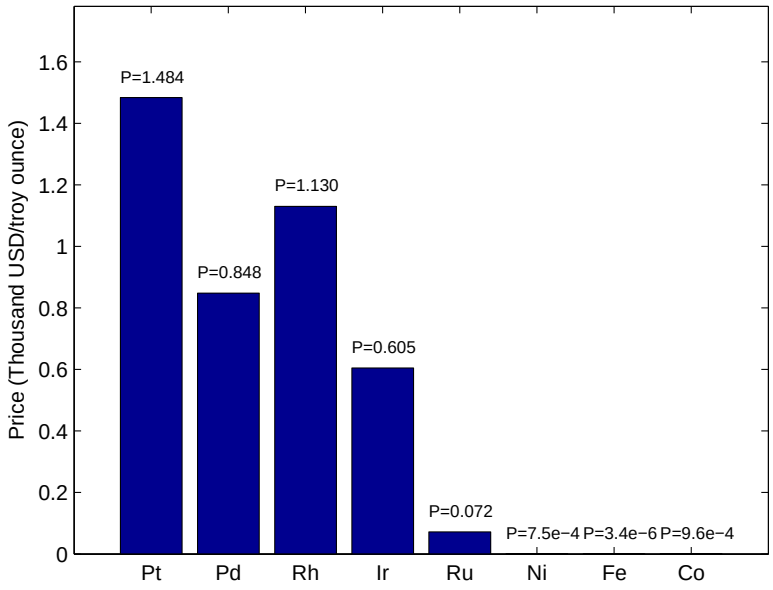

Figure 4: Price of different metals used in catalysts for steam and dry reforming [41, 42, 43]

and among transition metals, Fe is the cheapest.

A summary of potential catalysts for solar reforming as well as the different characteristics associated with these catalysts is presented in Table 1. Overall, noble metal catalysts have higher activity and better durability in terms of susceptibility to sintering and carbon deposition than transition metal catalysts. However, transition metal catalysts cost significantly less. Thus, there is a trade-off between catalyst cost and performance.

Catalyst - Active Metal:	Ni, Fe, Co, Ru, Rh, Ir, Pt, Pd
Catalyst - Promoter:	Mg, Ca, Ce, La, Zr
Catalyst - Support:	Al_2O_3, SiO_2, ZrO_2, TiO_2, La_2O_3, CeO_2
Catalyst Activity (steam reforming):	$Ru \approx Rh > Ni \approx Pd \approx Pt > Co$
Catalyst Activity (dry reforming):	$Ru \approx Rh > Ir > Ni > Pt \approx Pd$
Catalyst Cost:	$Pt > Rh > Pd > Ir > Ru > Co > Ni > Fe$

Table 1: Summary of potential solar reforming catalysts and associated activity and cost

As discussed previously, catalysts are often used to avoid kinetic limitations. For the most part, reforming processes are reaction rate limited, where at given design parameters (i.e., residence time), the thermodynamic equilibrium limit for conversion is not reached. In this case conversion could be improved by altering the catalyst or changing the mass transfer properties through better mixing of reactants. In subsequent discussions, whether the reforming process is thermodynamically limited or reaction rate limited will be noted.

Now that the importance of reforming catalysts for reformer performance and design has been discussed, the different solar reforming systems previously studied will be presented.

3. Solar Reforming Systems

Most systems utilize direct dry and steam reforming with a few utilizing redox reforming. Dry reforming has been of great interest because it provides a method of converting undesired CO_2 into desirable fuels. Moreover, dry reforming can yield a product composition with lower H_2/CO ratios (as compared to steam reforming) which is preferable for feed used in other industrial processes like the Fischer-Tropsch process, and a higher CO content which

can be used for synthesis of oxygenated chemicals [44]. In addition, higher steam to fuel ratio (as compared to CO_2 to fuel ratio) is usually required in order to prevent carbon deposition [17, 44]. However, the dry reforming process does require a source of pure CO_2 which may not always be available. In general the reaction rate for either steam or dry reforming is approximately the same as the methane consumption is largely governed by the pyrolysis step [45]. Redox reforming breaks the steam and dry reforming into two reaction steps (a reduction and oxidation step). More on redox reforming and its potential advantages is discussed in Section 3.5.

Within the three different categories of solar reformers, the system can be either directly or indirectly heated. In most cases the reformer is directly heated which is defined herein as a system where the solar receiver and reactor form an integrated unit and the reactor is directly heated by the solar radiation. High temperatures are typically reached within the reaction site ($> 1000°C$), and the reforming processes in these systems are typically reaction rate limited. While not as common, there are few indirectly heated reforming systems. Indirectly heated reforming systems are classified herein as those systems in which the solar receiver and reactor are two separate units, and solar energy is used to heat a heat transfer fluid (HTF) that circulates between the two units. While these systems operate at lower temperatures, they do not pose a restriction on the reactor size since it does not have to fit inside the receiver. The larger reactor size increases the residence time which can be beneficial to fuel conversion and can balance out the impact of the lower temperatures. For the most part, unless otherwise noted, reformers discussed are directly heated systems.

In order to fully characterize these reforming systems, three aspects must be considered: (1) the solar collector/concentrator and how it is integrated with the chemical reactor (either directly or indirectly), (2) the catalytic element (i.e., what is used as the reaction site and what type of catalyst is used), and (3) the design of the reforming reactor where heat is collected and the actual conversion takes place (i.e., size, where it is solid or liquid, dense or porous, the residence time, etc.). Work on these types of reformers is discussed in more detail next.

3.1. Dry Reforming Systems

Dry reforming is of great interest because it converts CO_2 into useful syngas. There have been many different solar reformer studies that utilize dry reforming as the fuel conversion method. These systems will now be discussed in more detail.

3.1.1. Dry Reforming With No Catalyst

Catalysts are often used in solar reformers to achieve significant conversion at reasonable flow rates. However, some work on dry reforming systems without a catalyst has been attempted. These systems typically require very high temperatures. One such study was done by Dahl et al. using a fluid-wall aerosol flow reactor [46]. The fluid-wall aerosol flow reactor was composed of three concentric tubes (Figure 5). The innermost tube was a porous graphite tube, the middle was a solid graphite tube, and the outer was a quartz tube. Sunlight heated the center solid graphite tube which in turn heated the inner porous graphite tube. The reactant gases were fed through the porous graphite tube from the top. Argon was used as a carrier gas and was fed

into the annular region between the two graphite tubes. Argon was also fed in the opposite direction in the annulus between the solid graphite tube and the quartz tube to prevent oxidation of the graphite tube. The porous graphite tube that served as the reaction site had a 0.012m inner diameter and a length of 0.31m. The reformer was paired with a solar furnace. An

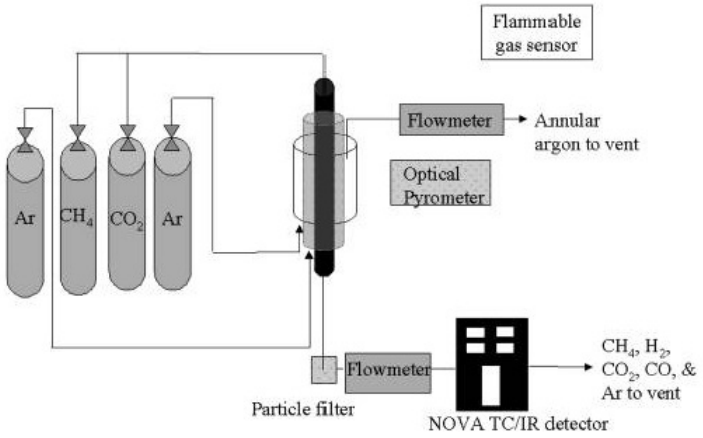

Figure 5: Schematic of experimental setup for fluid-wall aerosol flow reactor [46]

overall concentration ratio of approximately 4049 was achieved, resulting in temperatures between 1770° and 1860°C [46]. These very high temperatures allow for the dry reforming reactions to occur at reasonable rates without the use of a catalyst.

For the reforming tests, a CH_4:CO_2 of 2 was used. Excess methane was used in order to minimize the Boudouard reaction between CO_2 and graphite tube that is thermodynamically favored at temperatures above 1000 K [46]. The maximum methane conversion achieved was approximately 77% with a reported residence time on the order of 10ms [46]. Again, the relatively high methane conversion (although still lower than equilibrium) achieved

with the low residence time and no catalyst is due to the very high reactor temperatures.

Another study of dry reforming without a catalyst was done by Klein et al. [47]. In this system, a particle seeded receiver was used to perform dry reforming with methane. Carbon particles were used and were entrained within the reforming gas mixture. The particles were used as the reaction surface for the reforming reactions as well as the absorber element (as the particles absorb the solar radiation and transfer it to the reforming gas) [22]. The carrier gas for the particle was either Ar or CO_2 [47]. A schematic of the receiver is shown in Figure 6. The solar reformer was tested with primary and

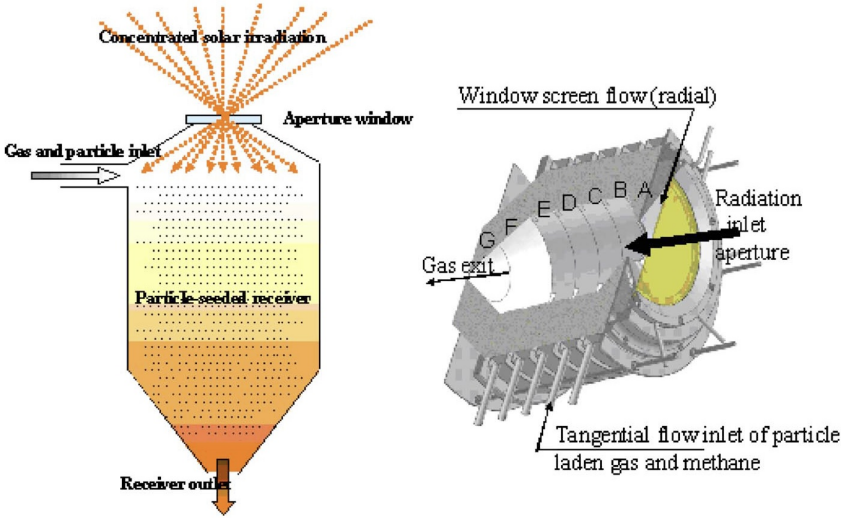

Figure 6: Schematic of particle seeded receiver [47]

secondary concentrators reaching a maximum solar flux of 3 MW/m^2 [47]. For the reforming tests, the CO_2 to CH_4 ratio was varied between 1:1 and 6:1, and the reforming temperature varied between 950° and 1450°C. The maximum methane conversion achieved was 90% with a reported residence

time of approximately 0.3 seconds [47]. The high conversion suggests that the carbon particles within the gas flow increase the reaction rate.

These studies show that without a catalyst, very high temperatures are required in order to speed up the reactions and achieve significant conversion. Alternatively, a catalyst can be used to achieve the same conversion at lower temperatures. Overall, there is a balance between the complexity of using systems with high concentration ratios (to achieve the high temperatures) and using a catalytic reactor. The subsequent studies discussed all utilize a catalyst.

3.1.2. Dry Reforming System using metal foam and porous ceramics [48, 49, 50]

Moving on to systems that utilize a catalyst, a lab-scale study of dry reforming was done using a porous absorber reformer with different absorbers and catalysts integrated with a solar-simulated Xe-arc lamp light [48, 49, 50]. A schematic of the experimental setup is shown in Figure 7.

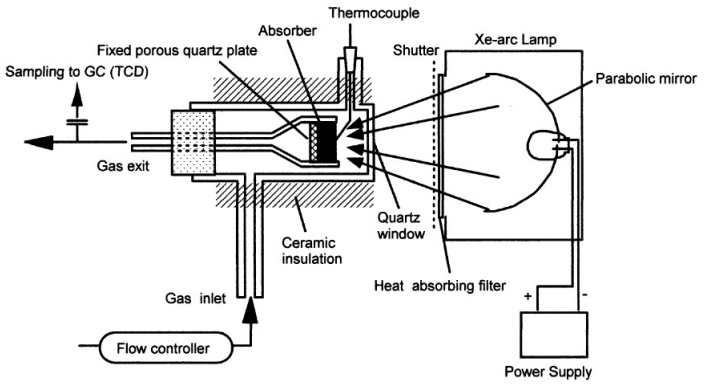

Figure 7: Schematic of experimental setup of solar reformer with porous absorber [49]

The reactor was a double walled quartz reactor tube and the absorber/reformer

was placed in the inner tube behind the quartz window (Figure 7). Solar fluxes between 150kW/m^2 and 350kW/m^2 (temperatures between 730°C and 1030°C) were achieved. Note that while solar fluxes are a large contributor to reactor temperatures achieved, the temperature is also largely dependent on the flow rates (i.e., convective heat transfer). Two different absorbers were used: metallic and ceramic. The metallic absorber consisted of a Ni-Cr-Al metal foam disk (Ni based alloy with 20-30% Cr and 4-7% Al). The disk was 30mm in diameter, 10mm thick, had a pore size of approximately 0.8mm, and a surface area of 2500 m^2/m^3. The ceramic absorber consisted of an alumina ceramic disk and had the same dimensions as the metallic absorber. For the catalyst, both supported and non-supported catalysts (Rh, Ru, or Ni) were used. The metal loadings were fixed to 7.3μmol-metal/cm^2 for the metallic absorber and 14.6μmol-metal/cm^2 for the ceramic absorber. The alumina support (if used) was 10 percent by weight. The dry reforming process was run for a CH_4 to CO_2 ratio of 1 and a total flow rate of 1dm^3/min (dm = decimeter).

Figure 8 shows that the alumina supported catalyst is better in terms of sustaining activity throughout the entire test [49]. It also shows that Ru is best in terms of maintaining activity for extended periods of operation [49, 51]. The alumina support was applied in two different ways and a comparison of the two methods is shown in Figure 9. Note that for this comparison the metal loading was fixed at 14.6μmol-metal/cm^2. Figure 9 shows that the alumina support application method with the γ-Al_2O_3 particle slurry is better in terms of the stability of the catalyst activity [49]. For comparison between the metallic and ceramic absorber, methane conversion over time

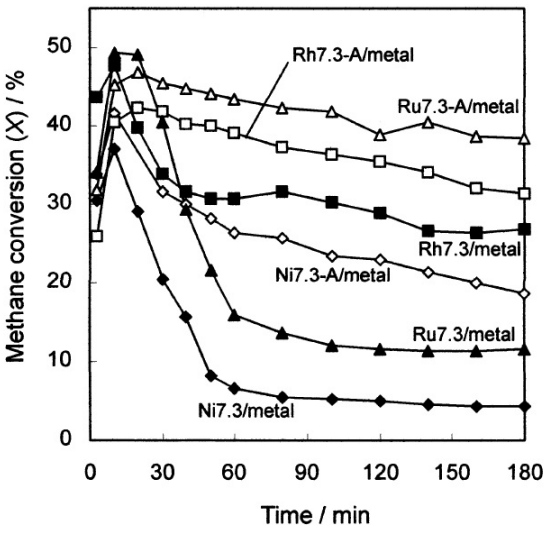

Figure 8: Comparison of catalyst activity over time [49]

for the two types of absorber with supported Ru catalyst is shown in Figure 10. Since the Ru with Alumina support had the most stable activity, it also had the highest chemical efficiency of approximately 50% and the highest methane conversion of 73% [49]. Figure 10 shows that the metal absorber achieves better conversion than the ceramic absorber under the same conditions [48, 49, 50]. The higher conductivity of the metallic absorber improves the temperature uniformity and hence the chemical efficiency; however, other factors could effect the latter including catalyst dispersion and radiative heat transfer so it is unclear which factors lead to better performance. Characterization of optical and thermal properties should be helpful in determining the reasons why the metallic absorber performed better [49]. Based on the volumetric flow rate of 1 dm^3/min given and the geometry of the absorber, the residence time was approximately 0.4s.

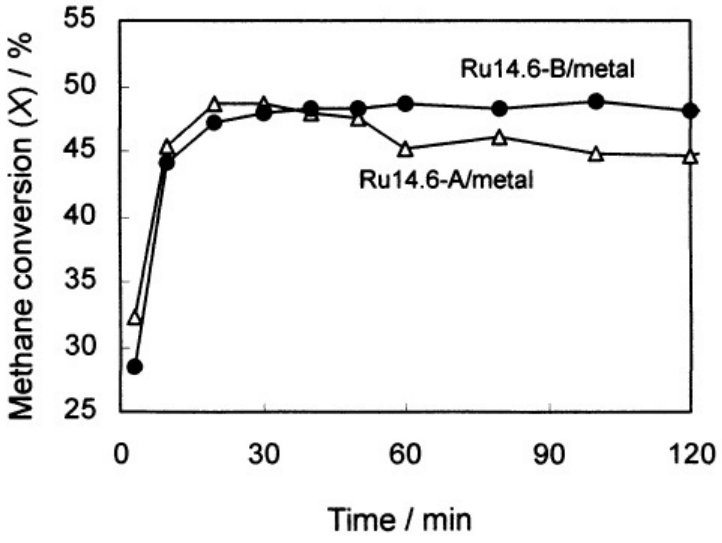

Figure 9: Comparison of Alumina support application processes: A - solution method and B - particle method [49]

3.1.3. CAESAR Project [52, 53]

One of the very first projects to examine high temperature solar reforming systems on a commercial scale is the CAESAR Project [52, 53]. In this project, a receiver named the direct catalytic absorption receiver (DCAR) was used for dry reforming of methane using a Rhodium catalyst. The DCAR was paired with a parabolic dish as shown in Figure 11. The parabolic dish was used to collect and concentrate the solar radiation. The receiver had a cylindrical steel housing with a quartz window (10mm thick) in its aperture. The absorber matrix (where the reactions occur) was mounted directly behind the window where it was illuminated/heated by the solar radiation. The dish used in this project had an area of 216m^2 and the receiver had a 60cm diameter aperture. The parabolic dish produced a maximum

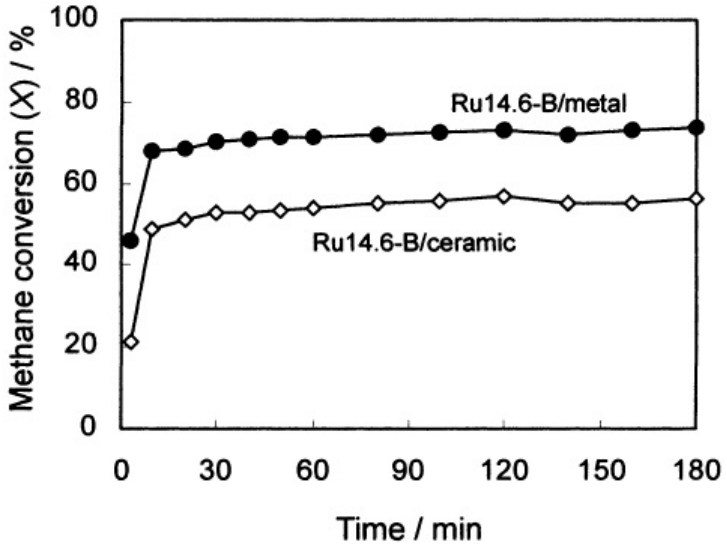

Figure 10: Comparison of metallic and ceramic absorber [49]

total incident solar power of 150 kW and flux densities up to $2MW/m^2$ and based on the areas given, had a concentration ratio of approximately 764, allowing DCAR to reach such high temperatures ($> 1000°C$). Note that the higher the concentration ratio, the higher the reactor temperatures. Although, as mentioned previously, the flow rate of the gases also has great effect on the reactor temperatures (i.e., decreasing flow rate increases reactor temperature). The reactants (methane + CO_2) flowed into the space between the window and the absorber matrix for heating. Next the gases flowed through the absorber where they were further heated and reacted as they come in contact with the catalyst.

The catalytic element in this reactor was an absorber matrix. For the CAESAR project two absorbers were constructed. Each consisted of a central disk and eight outer ring pieces. Figure 12 shows an expanded view of the

Figure 11: Setup of DCAR with parabolic dish in CAESAR Project [52]

absorber matrix. The absorber consisted of a central disk and outer ring pieces (as opposed to one large disk) in order to allow for different pore size distribution along the axial (gas flow) direction of the absorber between the center and outer ring pieces, which attempted to match the gas flow rate with the temperature distribution. The ceramic foam was made of 92% α-alumina and 8% mullite, with high thermal conductivity of 30W/mK [54]. The overall absorber had a diameter of 64cm, a thickness of 5cm, and a porosity of approximately 85% [55]. For the catalyst application, the absorber was first coated with a 6% by weight γ-alumina washcoat to provide an increase in surface area. After the washcoat, Rhodium was loaded on the absorber to approximately 0.2% by weight using incipient wetness. This technique involves dissolving the active metal in an aqueous solution and adding to the absorber the metal containing solution where capillary action draws the solution into the pores of the absorber. The absorber can then be dried and

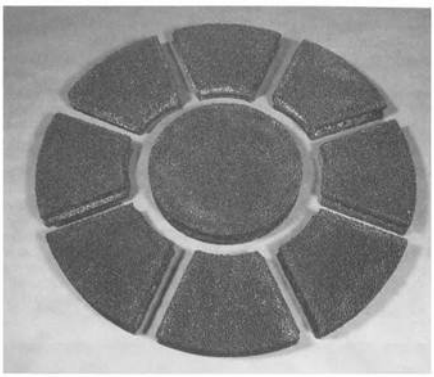

Figure 12: Expanded view of the absorber used in CAESAR Project [52]

calcined [56].

For the experiments, the DCAR was installed in the receiver test bed of a parabolic dish test facility and the dry reforming process was run with a CO_2 to CH_4 ratio of 1. The solar energy into the receiver was varied to obtain a more uniform solar flux distribution and therefore a more uniform temperature across the face of the absorber (radial direction). Experiments were run for a typical day and a cloudy day with irradiation being $520 - 590 W/m^2$ and $0 - 590 W/m^2$, respectively. The inlet flow of CH_4 (and the CO_2 flow rate to maintain a 1:1 ratio) was changed throughout the test run between 0 and 75 m^3/hr. The steady state temperatures at the center of the absorber was between 750°C and 1100°C for a typical day. The temperature variation in the axial (gas flow) direction was reported to be approximately 200 degrees and not as much temperature variation in the back half of the absorber [55]. In addition, it was found that the gas temperature initially increased rapidly over the first few centimeters of the absorber and then equilibrated with solid temperature between 1.4 and 2.3cm from the front

surface [55]. This suggests that most of the heat transfer (both convective between solid and gas and radiative/conductive within the solid) occurs in the front half of the absorber. Therefore, it seems that while the extra length in the axial direction is beneficial for conversion, it is not necessarily needed for the heat transfer aspect.

The best reformer performance yielded a chemical efficiency of approximately 46% and a methane conversion of approximately 66% [52], achieved with a total incident solar input of 64.1kW (concentrated solar flux multiplied by area) and a reactant gas flow rate between 15 and 35m^3/hr [52]. The product of the reformer includes H_2, CO, CO_2, and H_2O. Taking the reactor size to be the absorber size, the thickness of the absorber divided by the range of space velocities (for the best performance) is used to calculate a residence time of approximately 2-4 seconds. Rh performed well in terms of avoiding carbon formation. However, it was discovered that the catalyst was not dispersed uniformly within the absorber, and it experienced sintering during the experiments which led to significant deactivation [52, 57, 55]. There was also significant sintering of the alumina washcoat. The absorber matrix also experienced material degradation (cracking and layer separation) due to the high temperatures [52].

Further work on a solar dry reformer system similar to the CAESAR project was done in the SOLASYS project [16]. A schematic of the solar reformer is shown in Figure 13. The SOLASYS system was tested at the Wiezmann Institute of Science in the power range of 100-220kW. The reforming tests yielded temperatures of 760°C with methane conversions close to equilibrium [22]. While the SOLASYS project focused on dry reforming,

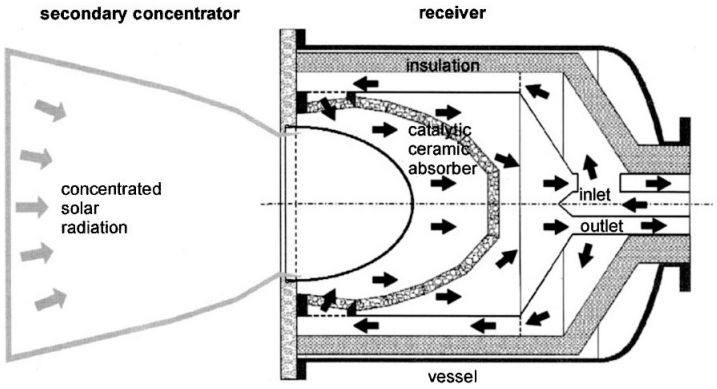

Figure 13: Schematic of solar reformer for SOLASYS Project [16]

it was also proposed for use in steam reforming [21].

3.1.4. Dry Reforming with Honeycomb Absorber [58]

While the previous studies have utilized a porous disk type absorber, there have also been studies comparing the performance of a honeycomb and porous disk absorber within a directly heated dry reformer [58]. In the study by Levy et al. a catalytic absorber was placed in a bell jar and then heated using a solar furnace. The furnace setup was similar to ones described previously: a heliostat (area = 96m^2) collected and reflected the solar radiation onto a spherical concentrator (diameter = 7.3m) which then concentrated the solar radiation onto the receiver reactor. From various measurements the furnace used can attain a concentration ratio over 11,000 suns [58]. The bell jar receiver was made of fused silica and enclosed the catalytic absorber (Figure 14). The bell jar was placed in a stainless steel housing and its sides were insulated with alumina wool.

The catalytic element in this system is the absorber. Both a honeycomb

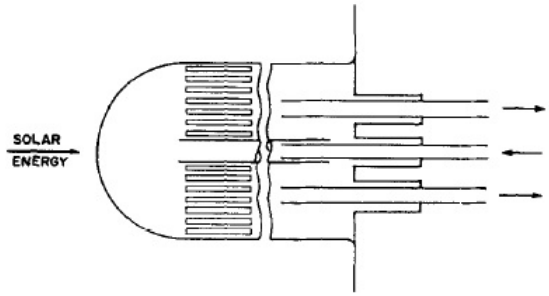

Figure 14: Schematic of transparent bell jar reactor [58]

and a porous disk absorber were used in order to compare their performance. Both absorbers were made of cordierite. With the honeycomb absorber, the square holes within the disk were 4mm in size with a 0.5mm wall thickness. The porous disk absorber had a porosity of 10 pores per inch. Two different thicknesses of honeycomb absorber were used (12 and 25mm), and a 35mm thick porous disk absorber was used. All absorber disks had a diameter of 14cm. Rh catalyst supported by alumina was used as the catalyst. To apply the catalyst, the absorber disk was first coated with an alumina washcoat. Then the active Rh was deposited onto the washcoat. The two types of absorbers lead to several differences including how radiation is absorbed and how heat is distributed within the reactor, how heat and mass transfer occur, and the gases come in contact with the catalyst. These differences can in turn affect the performance of the reformer.

Dry reforming tests were run between 700°C and 900°C with a reported CO_2 to CH_4 ratio of approximately 1.3 (i.e., an extra small amount of CO_2 was fed). It was found that the temperature differences across the honeycomb absorber (radial direction) were smaller than those for the foam ab-

sorber. Not as much temperature data was reported for the axial direction; however, the outlet temperatures of the honeycomb absorber are higher than that of the porous disk absorber even with lower solar inputs. Moreover, the temperature difference between the absorber and gases at the exit was smaller for the honeycomb absorber which indicates that there is more efficient energy absorption by the reacting gases in the honeycomb absorber [58]. The honeycomb absorber yielded better performance (even though the porous disk absorber was thicker and allowed for higher residence time). The thicker honeycomb absorber gave higher methane conversion because of the higher residence time. Overall best performance was achieved with the 25mm honeycomb absorber with 266mg of Rh at around 750°C and a solar input of 574 W/m^2 [58]. In this case, methane conversion achieved was approximately 67% at a chemical efficiency of approximately 65% [58]. Based on the size of the absorber, the residence time is calculated to be approximately 500ms. While it would seem that the honeycomb absorber yields higher conversion mainly due to the higher overall temperatures, a more detailed study of the temperature/radiation distribution (particularly in the axial direction) would be useful in determining the exact cause of the better performance.

3.2. Dry Reforming - TCRR System [59]

Another early proof of concept study was done by Anikeev et al [59] where dry reforming of methane was performed using a thermochemical catalytic receiver/reactor (TCRR) in conjunction with the high flux solar furnace. A schematic of the furnace is shown in Figure 15. Essentially a heliostat was used as the collector that concentrates the solar energy onto a secondary concentrator, which then focuses the solar radiation onto the TCRR (at

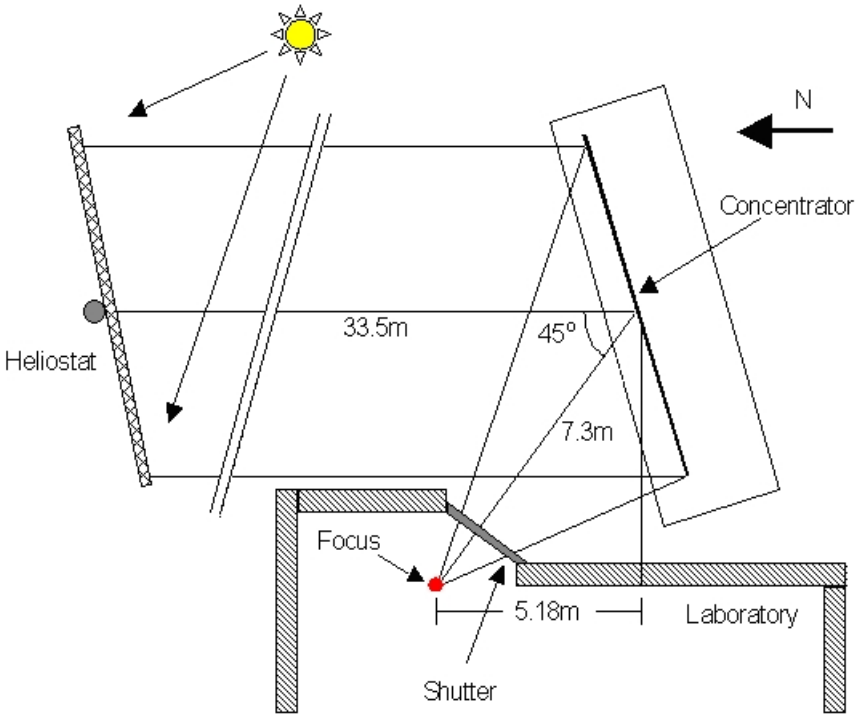

Figure 15: Schematic of solar furnace used with TCRR [60]

the focal point in Figure 15). The heliostat had an area of $57m^2$ and the secondary concentrator had an area of $42m^2$ [60]. The solar furnace has a peak concentration ratio of 4800 and was able to produce solar flux densities up to $5MW/m^2$ [60].

The TCRR itself contained a conical shaped receiver with a cylindrical shell absorber surrounded by a glass wall inside the receiver. The gas flow and radiation were essentially radial in this case, through the cylindrical shell absorber. A schematic of the gas flow is shown in Figure 16.

The catalytic element is the cylindrical shell absorber. The active metal and the catalyst support were ingrained within the ceramic material. For this

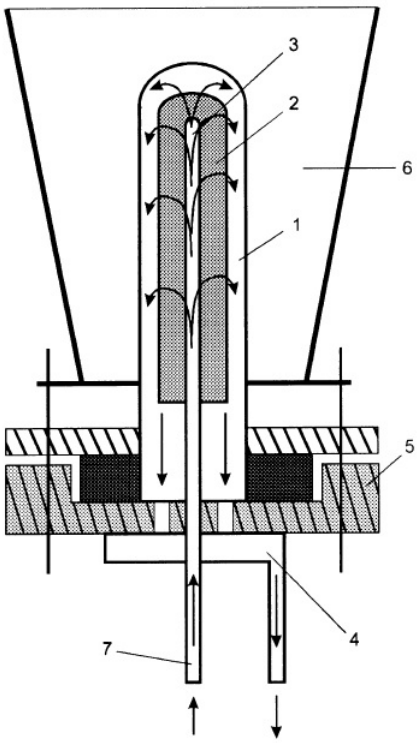

Figure 16: Schematic of gas flow within the TCRR: (1) - glass wall covering the absorber, (2) - porous cylindrical absorber, (3)/(7) - inlet pass for reactant gases to enter the absorber, (4) - outlet gas exit, (5) - base to fix glass cover and absorber, and (6) - conical solar receiver [59]

project, two absorbers were made: one with Ni-Cr as the active metal and one with Ru as the active metal. Both absorbers had an overall diameter of 30mm and a length of 218mm. Reforming occurs as the reactants flow radially through the shell.

For the reforming tests, CO_2 to CH_4 ratios between 1:1 and 3:1 were used (while keeping the total flow rate fixed at 3.6 l/min). The solar power ranged between 1.5 and 2.75kW (concentrated flux between 300 and 500 kW/m^2) which yielded reforming temperatures between 650 and 850°C. The temper-

ature distribution along the absorber was also measured and it was reported that the absorber temperature stabilized as the point moves inside away from the front surface [59]. The temperature variation within the absorber was approximately of the same order of magnitude as that observed in the CAESAR project. Moreover, the solar flux only changed the absolute value but not the temperature profile itself [59]. The best performance yielded a maximum methane conversion of approximately 60% and a maximum chemical efficiency of approximately 30% for the Ni-Cr absorber [59]. No data was given for the Ru absorber. The study reports that the radial supply of reactants and discharge of products are such that there is sufficient contact time for the reactions to occur; however, not enough information is given to calculate an actual residence time. The activity of the catalyst did not change during the tests and no coke deposition was reported [59]. The experiment showed the feasibility of a TCRR; however, the operating temperatures were purposefully restricted to lower values (as compared to other systems like the CAESAR project) for fear of deactivating and degrading the catalytic element.

3.2.1. Dry Reforming with Metal Oxide Catalyst in Liquid Bed [61, 62]

Most dry reforming systems use a catalytic element applied to a solid absorber which is directly heated by solar radiation. There have also been studies on a reformer that utilizes a directly heated fluid bed. With the solid absorbers discussed previously, there is not necessarily temperature uniformity within the reactor which can be detrimental to the reactor performance. Moreover, for solar reformers in general there is often fluctuating temperatures due to the fluctuating incident solar radiation. One potential solution

to these problems is to use a fluid bed as the fluid can have a much higher heat capacity that the solid absorber (2-3 times higher), which leads to circumvention of rapid temperature changes due to fluctuation of solar insolation as well as more uniform temperature within the reactor by natural or forced convection of the fluid [62]. In the liquid bed case, the reaction site is heated by the conduction through the reactor wall (which is being directly heated by the solar energy) rather than by the solar radiation itself (as is the case in the solid absorber reformers discussed previously). This difference also contributes to the temperature distribution as well.

Gokon et al. performed a study of a dry reformer with a molten salt/iron oxide solution as the catalytic element [61]. The molten salt containing FeO powder was placed in the reaction vessel and the reactant gases (CH_4 and CO_2) were sent through solution, which was heated by the solar radiation. The molten salt's relatively high heat capacity minimizes the temperature fluctuation even when solar insolation values vary [61]. The melting point of molten salt ($\approx 710°C$) is lower than the reforming temperature and phase change is avoided [61]. In this particular study, the reactor tube was tested with a infrared furnace as shown in Figure 17. Essentially the reactor tube with the molten salt/FeO solution was heated by the infrared furnace and the reactant gases were sent into the reactor tube from the bottom and then collected at the top for analysis. The reactor tube was made of stainless steel and had a 30mm diameter and a length of 300mm.

The catalytic element for this reformer system involved two components: the FeO catalyst and the molten salt. The FeO catalyst was prepared by reducing analytical grade FeC_2O_4. The FeC_2O_4 powder was first heated in a

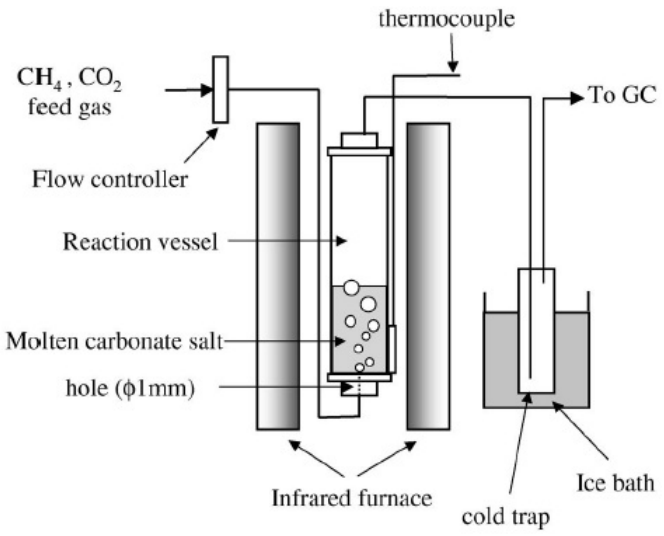

Figure 17: Schematic of experimental setup for molten salt reactor [61]

N_2 gas stream at 650°C for 1 hour and then reduced under a H_2 gas stream at 750°C for 15 minutes to obtain the FeO catalyst. The molten salt contained a 50-50 mixture of K_2CO_3 and Na_2CO_3. For the catalytic element as a whole, 20g of the FeO powder and 20g of the molten salt were mixed and then placed in the reaction vessel.

For the reforming tests, the reaction vessel with the molten salt/FeO catalyst was first heated by the infrared furnace to a temperature of 950°C. Then the CH_4/CO_2 mixture (1:1 ratio) was sent into the reaction vessel at various flow rates (between 50 and 400ml/min). The flow rate affected the product composition. For higher flow rates (200 ml/min), the products were CO, H_2, and H_2O (mole ratio of approximately 3:1:1) [61]. For lower flow rates (50ml/min), the reforming product yielded a CO to H_2 ratio (approximately 1.4) closer to theoretical dry reforming [61]. This difference in reforming

products can be explained by the residence time. The residence time is calculated to be between 2-9s for the range of flow rates. This residence time is based on the volume of the liquid bed which is estimated based on the density of the molten salt. No actual conversion metrics were reported for this study.

Kodama et al. used a similar reactor design [62]. In this study however, Ni, Fe, Cu, and W supported on Al_2O_3 were used as the catalyst. The metal content of the supported catalyst was approximately 20% by weight. The molten salt was again a 50-50 mixture of K_2CO_3 and Na_2CO_3. The molten salt and supported catalyst were mixed (weight ratio not constant in tests) and placed in the reactor tube. Total weight of salt/catalyst mixture ranged between 30g and 50g.

The experimental protocol involved testing three different aspects of the catalytic element/reformer operation: 1) the active metal, 2) the ratio of the weight of the salt/catalyst mixture to the reactant gases flow rate, and 3) the weight ratio of supported catalyst to molten salt. For each test, the reactor tube was heated in an infrared furnace to 950°C and a CH_4/CO_2 mixture (1:1 ratio) was sent into the reaction vessel at 200-800cm^3/min. Again, based on the volume of the liquid bed, the residence time is calculated to be between 2 and 6 seconds. Ni was found to be the most active in terms of methane conversion, with CO, H_2, and H_2O as products [62]. Testing revealed that the methane conversion increased linearly with the weight of salt/catalyst mixtures to gas flow rate ratio (ratios between 0.05 and 0.25g-min/cm^3 were tested). Figure 18 shows that the methane conversion increases linearly with catalyst/molten salt ratio at fixed total weight of the catalyst plus molten

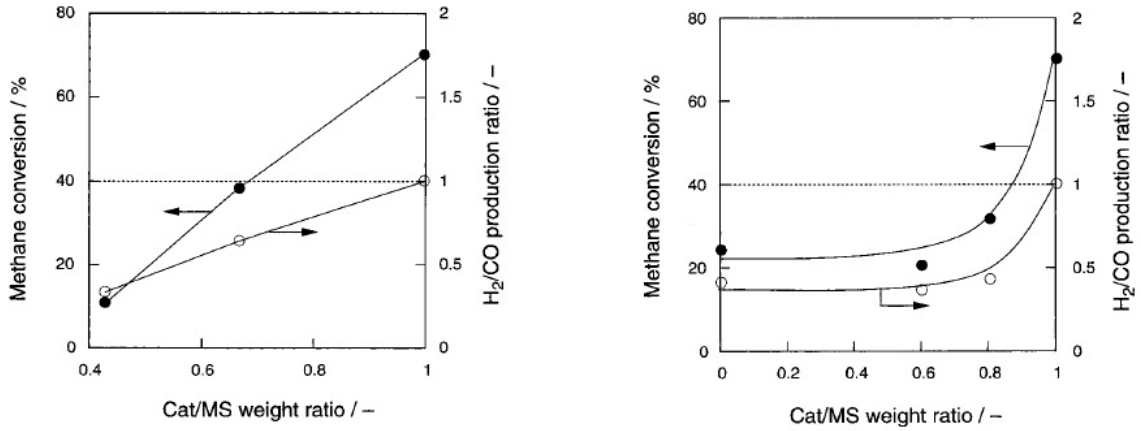

Figure 18: Reforming results for varying catalyst/molten salt ratio: keep total weight constant (left) and keep amount of salt constant (right) [62]

salt mixture. As H_2 to CO ratio approaches the stoichiometric ratio, the catalyst/molten salt ratio increases. With fixed amount of molten salt constant, as the catalyst/molten salt increases the methane conversion increases for ratios higher than 0.8 [62]. Moreover, temperature measurements along the reactor showed that the temperature difference within the molten salt mixture was less than 10 degrees [62]. This temperature difference is much smaller than what has been achieved in the reformers with the solid absorber (see discussion of CAESAR project in Section 3.1.3). The much smaller temperature variation can be beneficial in terms of maintaining thermal stability and long term operation of the solar reformer.

3.2.2. Dry Reforming with Heat Pipe

In addition to utilizing solid absorbers or fluid beds, dry solar reforming studies have also been conducted utilizing a heat pipe. Under certain operating conditions such as high pressure processes, tube-type reactors might

be better suited than the solid porous absorbers discussed previously. However, heating reactor tubes with concentrated solar energy can be challenging due to the fluctuating solar fluxes and transient nature of solar systems [63]. Therefore one solution to this is to utilize a heat pipe. In a heat pipe type reactor, a liquid comes into contact with the hot surface of the heat pipe and evaporates. The vapor travels along the the heat pipe to the cold interface and condenses back into liquid. Through the condensation process, energy is realized providing the heat source needed for the reactor.

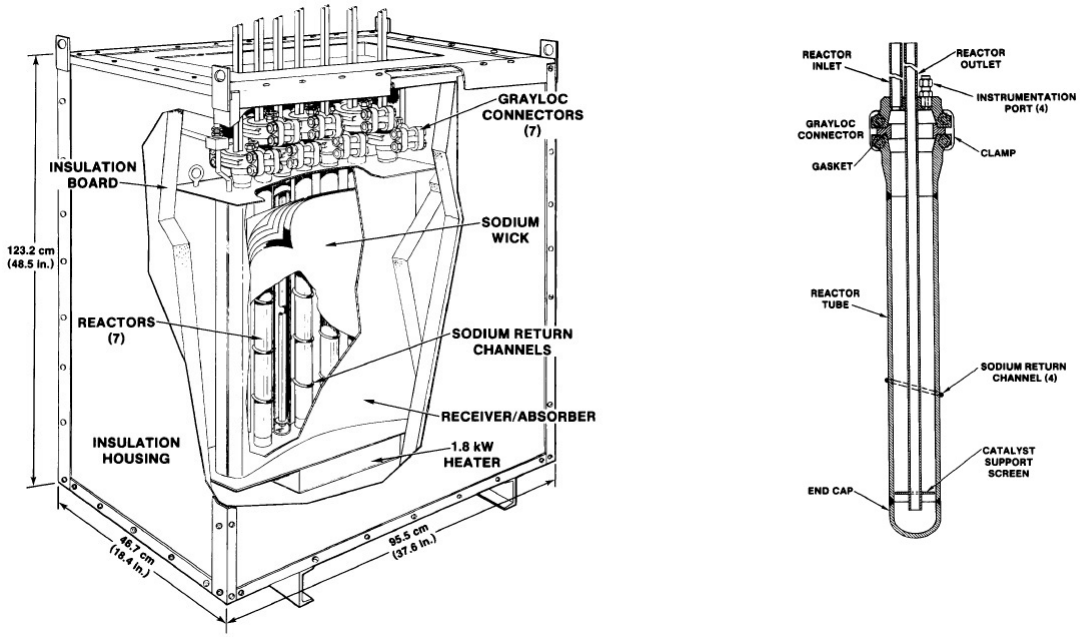

Figure 19: Schematic of sodium reflux heat pipe receiver reactor system (left) and individual reactor tube (right) [63]

While solar heat pipe reformer systems would be considered indirectly heated due to the decoupling of the receiver and reactor, Diver et al. used an integrated sodium reflux heat pipe receive reactor system [63], and thus,

is classified in this paper as a directly heated system. In this solar reformer, seven reactor tubes were placed inside an insulated and evacuated metal chamber containing sodium (Figure 19). The liquid sodium contained in the evacuated chamber is evaporated by the solar radiation on the chamber surface facing the solar collector, and is condensed on the reactor tubes inside the chamber while releasing the heat of vaporization to the reactor tubes. Passive techniques (wicks) were used to return the liquid sodium to the evacuated chamber [63].

The reforming catalyst used was 0.5 wt% rhodium supported on gamma alumina pellets. The pellets were 3.2mm in diameter. The reactor tube was schedule 40 Inconel 600 pipe with a 4.83cm outer diameter and a 4.12cm inner diameter. No length for the reactor tube was reported. The reformer was tested in a solar furnace. The reactor temperatures were between 650° and 800°C, achieving methane conversion between 40% and 70% [63]. Moreover temperature measurements within the receiver along the length of the reactor tube showed that the temperature variation was approximately 15 degrees [63]. Similar to the liquid bed reformers, the temperature variation is much smaller than that of the solid absorber type reformers which can be beneficial for long term operation and stability. The reactor experiments were stopped prematurely due to operational failure with the sodium evaporator [63]. Moreover, this design maybe not be suitable for long term operation due to the flammability of sodium vapors [22].

Another dry reforming system using a heat pipe was also developed using air as the heat transfer medium [64]. Lab scale experiments of this reformer have been performed in a solar furnace to show feasibility [22]. Moreover, a

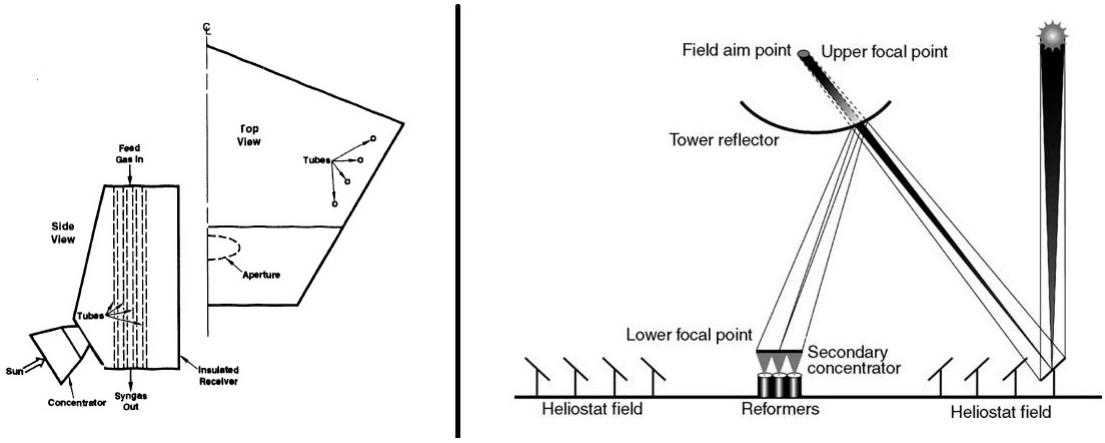

Figure 20: Schematic of heat piper receiver reactor system using air as heat transfer medium (left) and "beam down" solar receiver reactor concept (right) [64, 65]

480kW reformer has also been developed [66] (Figure 20). In this reformer, the cavity receiver consists of eight reformer tubes and the reformer was designed to produce syngas at 800°C. Each reformer tube is 4.5m long and has a 2.5 inch diameter. Due to the large size of the reformer, a "beam down" receiver concept (Figure 20) is used to integrate the reformer and solar receiver [65]. However, this design is still in the conceptual stage and has not been tested experimentally [22].

3.2.3. Dry Reforming - Summary and Comparison

Overall there have been a number of different studies on solar dry reforming. The dry solar reformers utilize either a porous ceramic, reactor tube with liquid bed, or heat pipe/reactor tube system for the integration of solar energy with the reaction site. In most cases, a noble metal catalyst is required in order to ensure the long term stability of the catalyst at the higher reforming temperatures. Comparison among these different systems shows that the

porous ceramic absorber systems tend to yield the highest conversions. However, these systems also have the largest temperature variations within the reactor which can lead to material degradation over time due to the thermal stresses associated with the temperature variation. The liquid bed and heat pipe reactors offer a much smaller spatial temperature variation but also a lower methane conversion. The smaller spatial temperature variation can be due to the higher higher heat capacity of the liquid bed. Moreover, how the reaction site is heated (by solar irradiation in solid absorber reformers and by conduction through reactor wall heated by solar radiation with liquid bed reformer) can greatly affect the spatial temperature distribution as well as the magnitude the reactor temperatures. The lower conversion can be due to the reactor temperatures as well as how the gases come in contact with the catalyst and the associated mass transfer properties. Moreover, there is most likely higher pressure drops in the longer tubular type reactors than the relative thin porous ceramics. In the end, there is a balance between the smaller temperature variations that can be achieved by the tubular type reactors with a liquid bed or utilizing a heat pipe and the higher methane conversions that are achieved by the porous ceramic absorber type reformers.

3.3. Steam Reforming Systems

Moving on from dry reforming systems, steam reforming systems are discussed next. As mentioned before, higher steam to fuel ratios are required to minimize carbon deposition and the steam reforming reaction yields a higher CO/H_2 ratio (as compared to dry reforming) which is not as desirable for feeds used in other industrial processes [17, 44]. However, steam reforming is still a popular method because steam is usually more readily available than

CO_2.

3.3.1. Steam Reforming - DIAPR System [57]

A directly heated solar reformer that utilizes a Ru/Al_2O_3 catalyst promoted with Mn oxides was studied by Berman, et al. in which a directly irradiated annular pressurized receiver (DIAPR) was used as the receiver reactor (Figure 21) [57]. The DIAPR could be used in conjunction with a

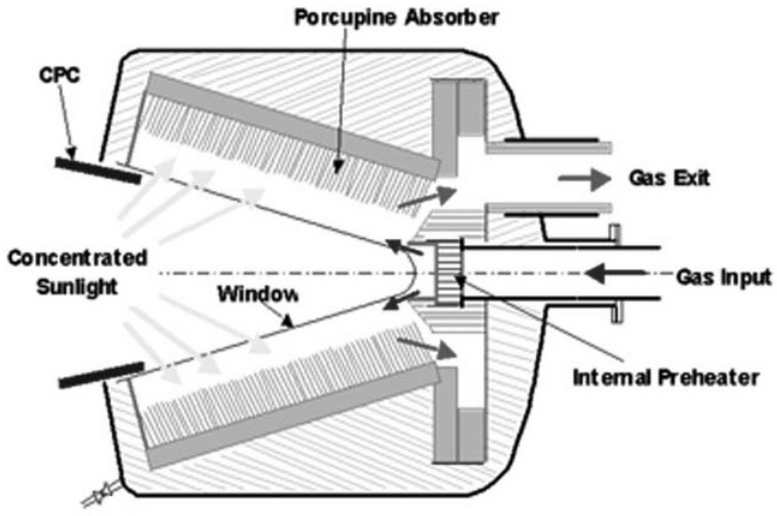

Figure 21: Schematic of a DIAPR solar reformer [57]

field of heliostats or in a parabolic dish similar to the setup with the CAESAR project discussed previously. Within the DIAPR system there was a secondary concentrator which further concentrated the radiation it received from the solar field (Figure 21). The absorber was a porcupine unit consisting of a large number of ceramic pins. The reactant gases flowed through the directly irradiated porcupine absorber around the individual pins as shown in Figure 22.

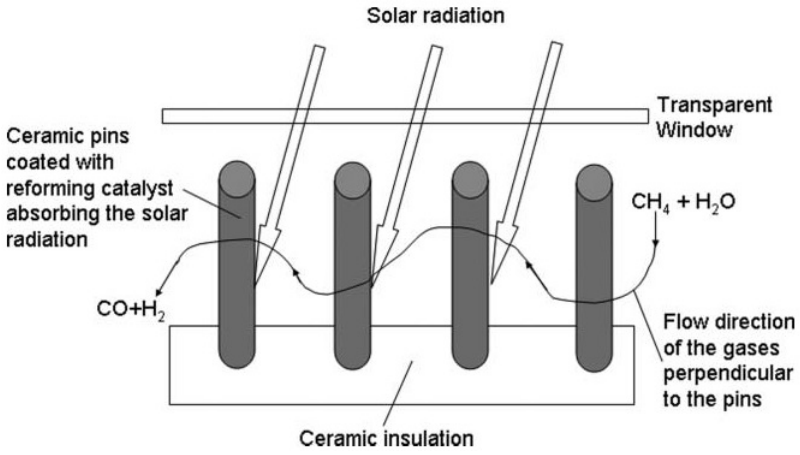

Figure 22: Schematic of gas flow within porcupine absorber [57]

The catalytic element was the porous ceramic pins in the absorber. Each pin was 40mm long and had a diameter of 3mm. The ceramic pins were made of sintered alumina (99.7% Al_2O_3). The catalyst was Ru/Al_2O_3 promoted with Mn oxides. The support wash coat was almost 10-20% of the pin weight, and Ru was approximately 5-10% of the washcoat weight [57].

Individual ceramic pins were tested first for catalyst activity and stability. A piece of the catalyst coated pin (approximately 1cm in length) was placed in a ceramic reactor (diameter = 12mm, length = 1300mm) [57]. The reactor was heated to 500°C-1100°C. Methane conversion using a fresh catalyst and catalyst that had been used for for 506 hours at 1100°C were compared (Figure 23). To prevent coke deposition during sample testing, the steam to methane ratio was 2.5 and the flow rate was 290cm^3/min. Figure 23 shows that the activity of the catalyst did not decrease significantly even after long periods (Ru with alumina catalyst without the Mn oxides tests showed that the activity greatly decreases at high temperatures. The addition of the Mn

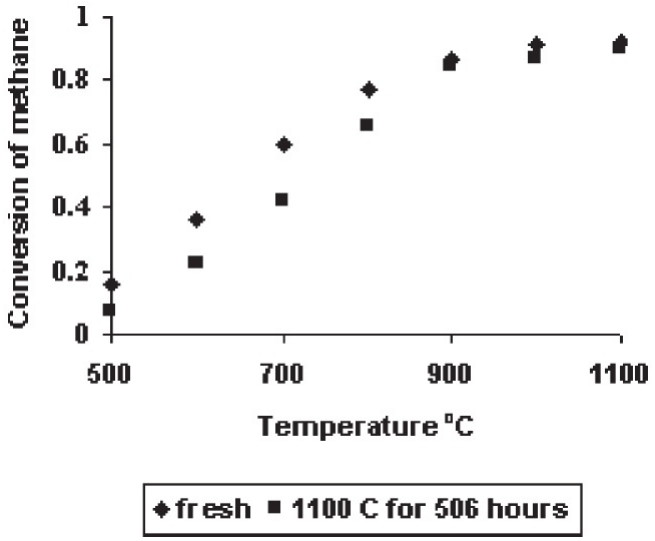

Figure 23: Comparison of activity of fresh catalyst and used catalyst - steam reforming of methane [57]

oxides improved the dispersion of Ru and decreased the rate of sintering of the catalyst) [57]. Reforming products included CO, CO_2, and H_2 with a molar H_2/CO ratio of 4 and a molar H_2/(CO+CO_2) ratio of 3.

Berman et al. used the same setup to test steam reforming of biogas (65% CH_4 and 35% CO_2). This can be thought of as combined steam and dry reforming of methane, and potentially reducing the danger of carbon deposition but changing the H_2/CO ratio of the product [57]. Reforming tests were run at a steam to carbon ratio of 2.5 and a flow rate of 446cm^3/min. Results are shown in Figure 24 for a fresh catalyst and catalyst that had been calcined for 129 hours. Methane conversion was much lower as compared to the pure steam reforming process. The lower methane conversion is most likely due to the lower contact times of the gases with the ceramic pins as the flow rate in the biogas case is nearly two times that of the pure methane

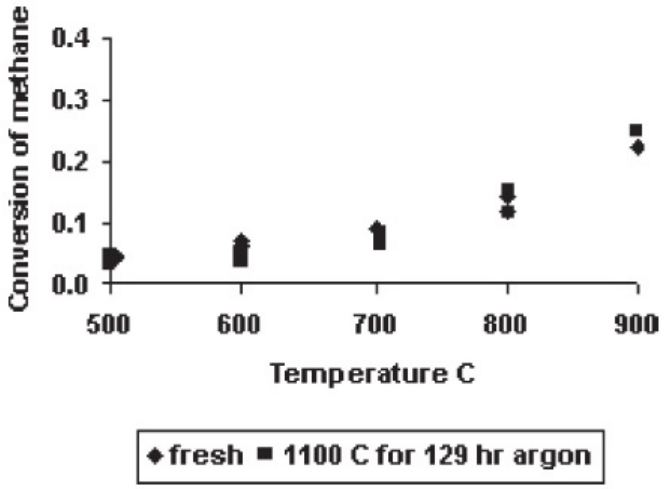

Figure 24: Comparison of activity of fresh catalyst and used catalyst - steam reforming of biogas [57]

case. The contact times were reported to be between 0.1-1s [57]; however, not enough information is given to determine the exact contact times for each case. Moreover, comparing the data for fresh and used catalyst, the difference in performance is not as large for the biogas case (same steam to methane/steam to carbon ratio for pure methane and biogas cases). This is most likely because, as stated previously, dry reforming has less disposition to carbon deposition, so the presence of CO_2 in the reforming process leads to better long term performance.

Ben-Zvi et al. developed a computational model of the DIAPR [67]. The model simulated the porcupine absorber (Figure 25). The reactive flow was modeled using the conservation equations. Moreover, instead of modeling each individual pin, an average medium approach was used where the effective distributed volumetric optical properties, flow resistance, and convec-

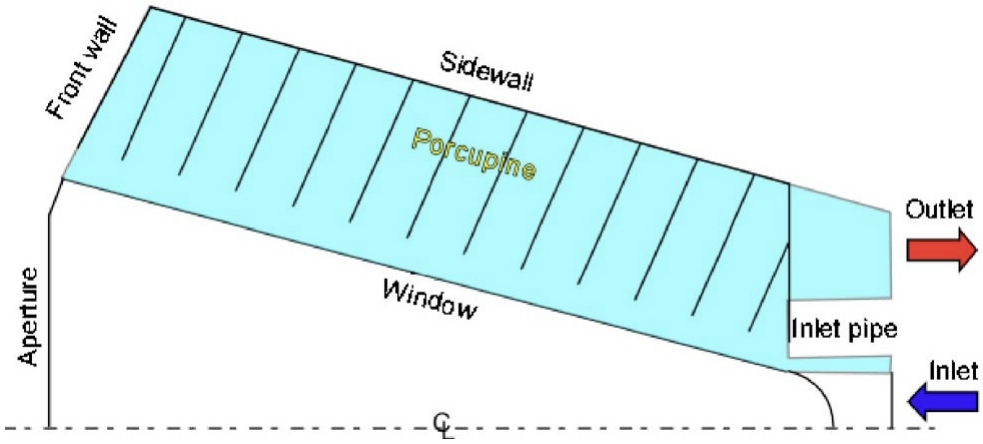

Figure 25: Schematic of DIAPR computational model domain [67]

tive heat transfer were assigned to each computational cell (control volume) within the porcupine absorber domain. The kinetic mechanism for the steam reforming was modeled using two global reactions calibrated to fit experimental results [68]. Parametric studies show that the pin length was very important in terms of ensuring contact between the gas flow and catalyst. The simulations showed that increasing the pitch reduced the fuel conversion, while increasing the receiver length favored conversion [67].

The porcupine absorber was also tested for with dry reforming to examine the effects of the gas pressure and flow rate [69]. The maximum methane conversion achieved was 85% [69]. Increasing the flow rate or pressure reduced the conversion, but the effect of changing the pressure was outweighed by the change in temperature or flow rate [69].

3.3.2. Steam Reforming - SOLREF Project [14]

This is a successor to the SOLASYS project discussed previously (Section 3.1.3). The SOLREF project developed a 400kW$_e$ reformer with a ceramic absorber (similar to the SOLASYS project) but for use with steam reforming [14]. A SiC foam coated with a 2% Rh catalyst was used as the solar absorber/reactor [14]. Methane conversions as high as 90% were achieved at temperatures of approximately 1100°C [14]. The SOLREF reformer is able to reach higher temperatures than its predecessor SOLASYS which leads to the higher methane conversion; however, as discussed previously, the product composition depends on the reforming process (higher H_2/CO and lower CO content for the SOLREF reformer). Not enough information is given to discuss the residence times or heat transfer effects in detail.

3.3.3. Steam Reforming - Packed Bed Catalyst [70]

In the study by DeMaria et al. a cavity receiver reactor was used. The reactor was paired with a 700W solar furnace. This furnace setup is similar to other setups discussed previously in that a heliostat (area of 4m^2) was used to collect the solar radiation and reflect it onto a parabolic reflector (diameter of 1.5m) which concentrated the solar radiation onto the receiver [71]. A cross section of the receiver is shown in Figure 26. It was made of AISI 304 stainless steel, and the catalyst was packed inside of the annular space.

For this study, the catalyst used was 10% Ni deposited on 2-3mm Al_2O_3 pellets. The reformer was run at atmospheric pressure and at 680 - 750°C. The steam to methane ratio varied between 1 and 3 for the various reforming temperatures. At 750°C, methane conversion was within 20% of equilib-

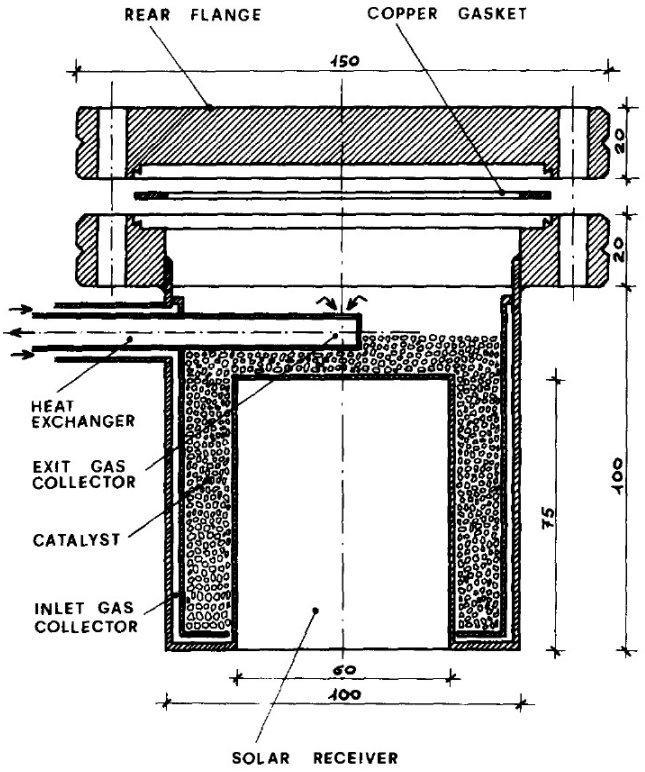

Figure 26: Cross-section of solar receiver reactor for DeMaria et al. study [70]

rium and the heating value of the reformed product was approximately 20% higher than that of the input methane [70]. Not enough information about the reactor volume size is given so residence times could not be calculated. Furthermore, no data was reported for the temperature distribution within the packed bed so it unclear if differences in performance from other steam reforming systems is due to heat transfer effects or other factors (catalyst, residence time, etc.).

3.3.4. Steam Reforming in a Tubular Reactor

Steam reforming has also been studied with a solar tubular reformer [72]. The reactor consisted of two concentric reactor tubes. The catalyst is packed between the inner and outer tubes of the reactor (Figure 27) and the steam and methane are fed into the reactor in opposite directions. The tubular reactor was directly heated by the solar energy (Figure 27). The reformer was tested with a 107m^2 dish concentrator and solar fuels were produced at temperatures of 850°C and pressures up to 20 bars [22]. An updated hexagonal

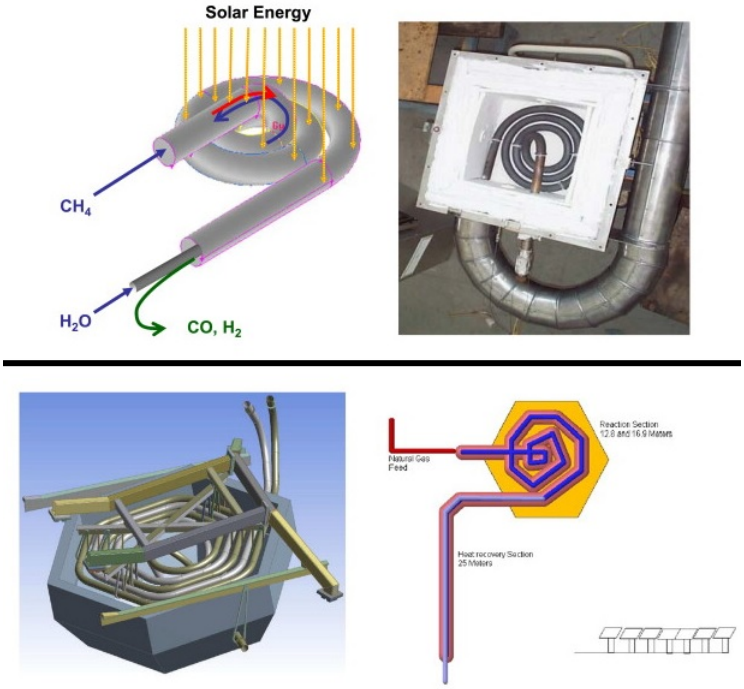

Figure 27: Schematic of CSIRO reformer: original (top) and updated hexagon design (bottom) [22]

shape, dual-coil reformer (DCORE) was also developed by CSIRO (Figure 27) and stable reactor temperatures and consistent hydrogen production was

reported [73, 74]. No detailed conversion metrics were reported.

3.4. ASTERIX Project [75, 64]

One of the commercial scale steam reforming projects is the ASTERIX system [75]. The ASTERIX system is an indirectly heated reformer. In this system, a heat exchanger steam reformer was utilized in conjunction with a Gas Cooled Solar Tower (GAST) [75]. The GAST was used to heat air up to 1000°C. The heat exchanger reformer contained a packed catalyst bed. Essentially the reactant gases were sent into the reactor tube which contained the packed catalyst bed, and the hot air was sent into the surrounding space for heat exchange between the reactor tube and the hot air.

As the reactant gases pass through the catalyst bed, they are heated from 500°C to 850°C by the time they reach the end of the bed [75]. Steady state tests were run for a variety of reforming temperatures (600-800°C). The steam to methane ratio was 3 [75]. Some steady state results are shown in Table 2.

Temperature (°C)	702	750	753	802	803
Pressure (bar)	7.6	7.7	7.7	6.1	7.8
CH_4 Conversion (%)	68	79	84	93	91

Table 2: Steady state test results for ASTERIX project [14]

Almost complete methane conversion (91%) can be achieved at approximately 800°C [14]. However, not enough detail is given about the size of the reformer or what exact catalyst is used. Note also that some of the methane that is not converted is recycled back into the reformer which can also contribute to the higher methane conversions.

Numerical studies for similar reforming systems have been done except with molten salt as the heat transfer fluid [76, 77, 78]. The reformer temperatures for these studies were much lower than the ASTERIX project (450-530°C). The maximum conversion achieved in these studies ranged between 15 and 21% [76, 78]. Simulations concluded that increasing the residence time, steam to fuel ratio, and inlet temperature increases the methane conversion, while increasing the operating pressure decreases the methane conversion [77]. Moreover, conversion was increased to between 54 and 69% when multiple reactor stages with hydrogen permeable membranes between each reactor stage was utilized [78].

3.4.1. Mixed Dry and Steam Reforming [79]

Mixed dry and steam reforming has already been discussed in the context of the DIAPR system. In a study done by Worner et al. a mixed dry and steam reformer was tested [79]. In the system shown in Figure 28, due to problems with the methanator, steam had to be injected into the reactor inlet stream which resulted in the reforming system being tested under mixed reforming conditions. The methane/CO_2/H_2O stream is sent into the receive reactor for reforming and the product gases are sent to the methanator system to create the methane. Between 25% and 100% of the products are recycled back into the reactor for further reforming. A schematic of the receiver reactor is shown in Figure 29. The receiver reactor is similar to other previously discussed systems (CAESAR, SOLREF, and SOLASYS projects).

Two different absorbers were fabricated and tested in this study. The first is made of an α-Al_2O_3 foam matrix with a porosity of 92%. The absorber was first coated with a 30% by weight of γ-Al_2O_3 washcoat. Next, Rh was

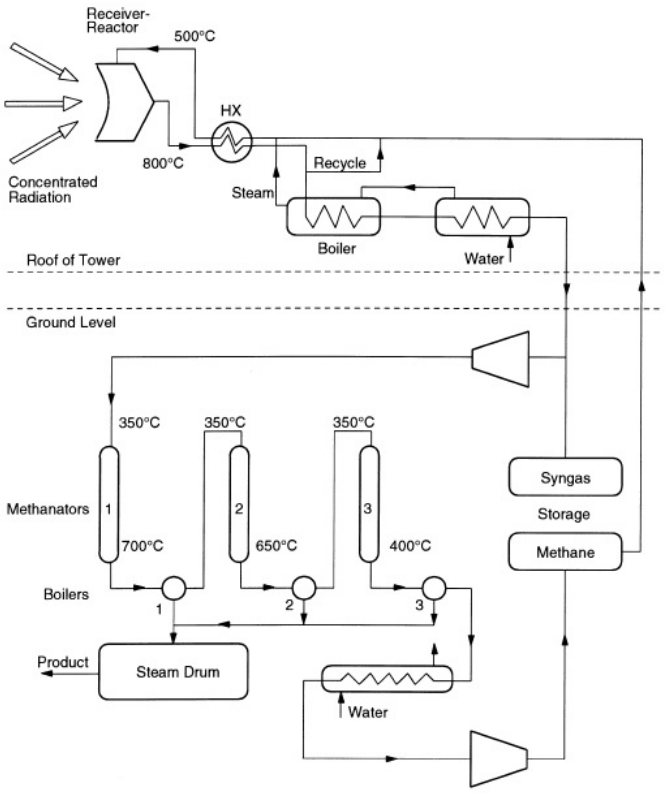

Figure 28: Reformer test loop of mixed dry and steam reforming system [79]

loaded onto the absorber. A catalyst loading of 11% by weight was used. The second absorber was made of a SiC ceramic foam with a porosity of 94%. The catalyst was applied in the same manner except the washcoat was only 10% by weight. The difference in material properties of the two absorbers can lead to differences in temperature (both magnitude and profile) due to the various heat transfer effects (different thermal conductivity, optical properties ,etc.) as well as differences in long term operational stability. The study did post-reforming analysis of the two absorbers and will be discussed later.

For the reforming tests the $(CO_2+H_2O)/CH_4$ ratio was approximately

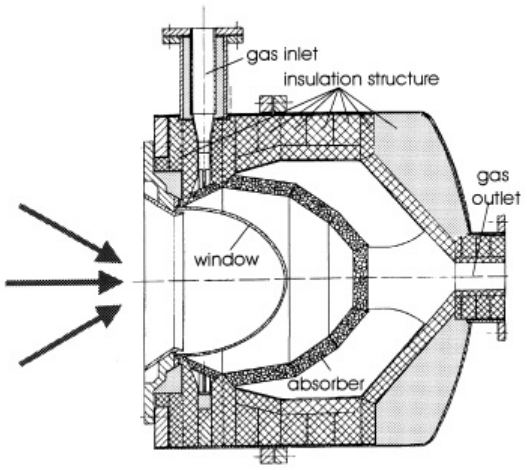

Figure 29: Schematic of receiver reactor for Worner et al. study [79]

1.8. The average absorber temperature ranged between 700°C and 830° and methane conversion of 84% was reached [79]. The average temperatures were slightly higher for the second absorber with a maximum of 858°C. Note that the difference in temperatures between the two absorbers can be attributed to the different absorber material properties (lower heat capacity for SiC). The higher temperatures, as expected, correspond to a higher methane conversion of 88% [79]. Since the reactants were recycled to have multiple passes through the reformer, the higher methane conversion is expected.

Cracks were discovered later in the alumina absorber but not in the SiC one. Both absorbers experienced some coking, and the catalyst on both absorbers experienced some poisoning which affected its activity [79]. Overall, this study demonstrated the feasibility of these reforming systems, however, the absorber systems would have to be modified in order to sustain the higher operating temperature conditions [79]. Moreover the comparison of the two

absorbers suggests that the SiC absorber is more suited for long term operation due to it higher thermal shock resistance.

3.4.2. Steam Reforming - Summary and Comparison

Similar to the dry reforming systems, the steam reforming systems utilized a number of different designs for the reaction site as well as integration with the solar receiver. The designs included the porous ceramic absorber, a fin type porcupine absorber, packed bed catalyst, as well as a heat pipe or heat exchanger type reformer. Highest methane conversion is achieved in the porous absorber reformer and heat exchanger reformer. However, these systems also have the highest operating temperatures which contributes to the highest methane conversion. The lower operating temperature systems did allow for use of cheaper Ni catalysts; however, the conversion achieved was lower due to the lower operating temperatures. Note that reaction rates for steam and dry reforming are approximately the same as the methane consumption is largely governed by the pyrolysis step [45]. More insight is also needed on the heat transfer effects to due to the different designs (i.e., packed bed versus porous ceramic) do determine their effect on the reactor performance.

3.5. Redox Reforming Systems

While direct steam or dry reforming of methane are the most common, some studies suggested using metal oxides for the same purpose. In redox reforming, the reforming process is divided into two main steps: the reduction

and oxidation step. The two main reaction steps can be written as

$$\text{Metal Oxide} + CH_4 \rightarrow \text{Metal} + CO + H_2 \tag{11}$$

$$\text{Metal} + \text{Oxidizer} \rightarrow \text{Metal Oxide} + \text{Oxidation Products} \tag{12}$$

In the above reactions the metal/metal oxide is the oxygen carrier. The oxidizer can either be steam or CO_2 which leads to either H_2 or CO as the oxidation products, respectively [80, 81].

Within the redox reforming system a number of different oxygen carriers can be used which allows for flexibility in design. Moreover, unlike in direct dry and steam reforming systems, an expensive noble metal catalyst is not required in order to ensure long term stability which in turn leads to lower costs. The redox reforming can be seen as essentially non-catalyzed reactions as the oxygen carrier acts as the "catalyst". In addition, steam redox can yield product compositions with more desirable (lower) H_2/CO ratios than direct steam reforming can.

3.5.1. Metal Oxide Methane Reforming + Water Splitting in a Redox System [10]

Kodama et al. investigated a steam redox reforming system that combined metal oxide reforming with water splitting [10]. The metal oxide reforming reaction is the same as the one shown in Eqn. 11 while the water splitting reaction is

$$\text{Metal} + H_2O \rightarrow \text{Metal Oxide} + H_2 \tag{13}$$

In most cases, the reduction reaction (converting metal oxide to metal) is

endothermic while the oxidation reaction (converting metal to metal oxide) can either be endothermic or exothermic depending on the metal/metal oxide pair used [80, 81]. In this study a quartz tube reactor with the metal oxide packed inside was used. The quartz tube reactor was heated by an infrared furnace (instead of a solar system) as shown in Figure 30. The tube reactor

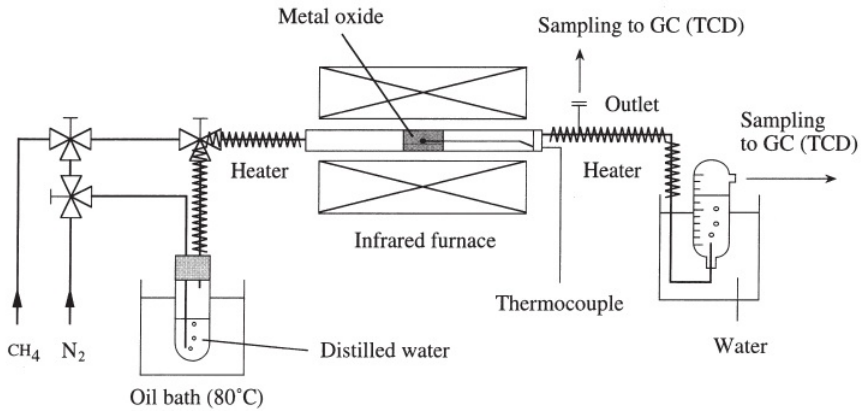

Figure 30: Schematic of experimental setup for redox reformer[10]

used in this study had a diameter of 8mm and a length of 240mm [10].

Seven different metal oxides were tested: SnO_2, In_2O_3, ZnO, WO_3, Fe_3O_4, MoO_2, and V_2O_5. SnO_2, In_2O_3, ZnO, and WO_3 were synthesized by thermally decomposing the appropriate hydroxides or H_2WO_4 in air. The hydroxides were created by hydrolysis of the appropriate metal chloride solutions. For the synthesis of MoO_2, MoO_3 was reduced using H_2. The MoO_3 was created by thermally decomposing $(NH_4)_6Mo_7O_{24}$ in air. The Fe_3O_4 was made by co-precipitation of Fe(II) and Fe(III) chloride mixed solution. The V_2O_5 was purchased commercially. The tungsten oxide was also supported by either SiO_2, Al_2O_3, or ZrO_2. The support was added by mixing the SiO_2,

Al_2O_3, or ZrO_2 powder in $(NH_4)_6(H_2W_{12}O_{40})$ solution and then evaporated and calcined. The metal oxides created are then packed into the reactor tube for testing.

For the reforming tests, the procedure was as follows: 1) the tube reactor was heated to the desired temperature (between 900°C and 1000°C), 2) methane gas was sent through the reactor for approximately an hour, 3) the reactor was allowed to cool to approximately 800°C, and finally 4) water vapor was sent through the reactor for one hour. The entire process (methane reforming + water splitting) was only run for the tungsten oxide. These reforming temperatures were chosen in order to achieve significant conversion of methane and metal to metal oxide conversion. For all other oxides, only the reforming part of the process was run. Considering only the reduction part of the process, V_2O_5 and WO_3 were found to be the best performing oxides in terms of methane conversion. V_2O_5, however, was not able to thermodynamically split water at sufficiently low temperatures. Therefore, WO_3 was used as the oxide for the reforming + water splitting process. As mentioned previously, the WO_3 was also supported with three different materials. As expected, the supported tungsten oxide performed better than the unsupported tungsten oxide in terms of methane conversion (due to the higher surface areas) with the ZrO_2 supported WO_3 having the highest methane conversion. The best performance for the reformer occurred at a reforming temperature of 1000°C with a total methane conversion of approximately 70% [10]. The reforming products include H_2, CO, CO_2, and H_2O with a H_2/CO ratio of approximately 2.27, which is fairly close to the stoichiometric ratio [10]. Not enough information is given with regards to

the size of the packed bed to determine the residence time.

3.5.2. Production of Zn + Metal Oxide Methane Reforming [82]

In the study by Steinfeld et al., a directly heated solar system that combines zinc production with methane reforming was investigated [82]. Zn is used in many industries such as the pharmaceutical and food industries [82]. The reaction in this reforming system is

$$ZnO + CH_4 \rightarrow Zn + 2H_2 + CO \tag{14}$$

While this system is not a true redox reforming process (as the oxygen carrier is not re-oxidized), it is included in this discussion because similar to redox systems it uses an oxygen carrier to convert the methane into syngas.

A receiver reactor called SynMet was used. A heliostat with an area of 51.8m^2 was used to collect and concentrate the solar radiation onto a secondary parabolic concentrator (area = 2.7m^2). The concentration ratio of this furnace can reach as high as 3500 suns [82]. The SynMet consisted of a cylindrical cavity with a circular windowed aperture where the solar radiation was directed (Figure 31). A stream of ZnO particles in methane is sent into the reactor cavity via a tangential inlet port located at the back of the reactor (Figure 31). As the flow moved axially forward through the cylindrical cavity, the particle stream formed a vortex flow towards the front where the window is being irradiated in a helical path. The products exited at the front of the receiver (Figure 31). The reactor cavity had a 10cm diameter and a length of 20cm [82]. The ZnO powder had a mean particle size of 0.4μm and was fed at a rate of 5g/min [82].

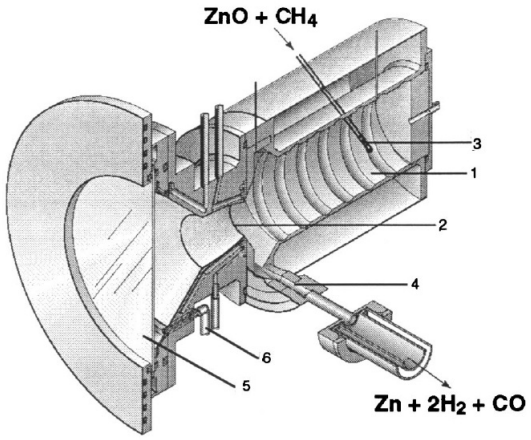

Figure 31: Schematic of SynMet: 1) cylindrical cavity, 2) aperture, 3) reactant gas inlet, 4) gas outlet, 5) aperture window, 6) auxiliary gas for window cooling [82]

Reforming tests were run between 730°C and 1030°C. To avoid particle deposition on the window, 5 - 25 times the stoichiometric amount of methane was added. The maximum methane conversion achieved was approximately 50% at 1030°C and at a reported residence time of approximately 3 seconds [82]. No axial temperature distribution data was reported.

A similar metal oxide reforming for magnetite and iron was also proposed and studied in [83]. While this study does discuss the potential of a chemical looping system (i.e., re-oxidizing the iron metal to get magnetite), the main focus was the production of iron in addition to syngas from the reduction of magnetite with methane [83].

4. Comparison of Different Solar Reforming Systems

Now that the various existing solar reforming systems have been discussed and characterized, a comparison will be presented. Solar reforming systems

have been divided into three main categories: dry reforming, steam reforming, and redox reforming systems. Within these different categories there are directly heated and indirectly heated reformers. In general with directly heated reformers, the reactor temperature is higher and the reforming process is reaction rate limited. In this case, the residence time is important and the size of the reforming element in the direction of flow matters, but the reactor should be housed inside a concentrator/collector and that could constrain the size. On the other hand, indirectly heated reformers tend to operate at lower temperatures because a heat transfer fluid is used to transfer heat between the concentrator and the reactor. Lower temperature imposes some thermodynamic limitations on conversion, which may require recycling some of the fuel to raise conversion.

For the purposes of upgrading fuels via solar reforming, reaction rate limited reforming systems are probably more desirable because in theory, if the reforming system is reaction rated limited, the performance of the reformer can be improved by using different catalysts or operating conditions. With thermodynamically limited systems, the performance is more difficult to improve due to the temperature limits of the solar collector/concentrator system. In addition to the reforming process, the design of the reactor + the solar collector/concentrator system must be considered. For directly heated systems, the receiver reactor is an integrated unit which means overall there are fewer components than the indirectly irradiated systems. Fewer components mean that a directly heated system may be easier to integrate with say a power cycle than an indirectly heated system.

A directly heated system, however, has a more complicated design and

more fragile components than an indirectly irradiated system which can lead to robustness issues and higher costs. Another point to make is that in a directly heated system, the size of the reaction site may be limited as the reactor and receiver are an integrated unit, while the reactor in an indirectly heated system can, in principle, be any size that is desired. A larger reactor in an indirectly heated system can lead to better performance (because of higher residence times), however, the larger reactors could be more expensive.

Redox reforming and dry reforming yield a lower H_2/CO ratio than steam reforming which is closer to what is desired for other industrial processes. Moreover, dry reforming can be used to convert CO_2 into a more useful fuel. In addition, steam reforming usually required higher steam to methane ratios to avoid coking. However, dry reforming does require a pure source of CO_2 which is not always readily available. At the high temperatures of solar reformers, often times a noble metal catalyst is required in order to maintain activity through extended periods of reforming. Past studies have shown that a Ru catalyst performed relatively well [57, 49]. However, since Ru is a noble metal, its cost is relatively high (as discussed in Section 2). Other catalysts such as Ni could be used to gain economic feasibility while sacrificing some performance. Redox reforming would provide an alternative as there is no true "catalyst" but rather an oxygen carrier is used. A number of oxygen carriers can be used which allows for flexibility [10, 80]. In redox reforming, the oxygen carrier must be re-oxidized after reforming, which makes the process more complicated. However, the oxidation step can be done in a number of ways and the oxidation step can lead to production of a pure stream of H_2 which can be useful for a number of different applications

[80].

In terms of the reactor design, it has been shown that porous metallic absorbers used as the catalytic element tend to achieve higher conversions due to the higher conductivity [49]. Honeycomb absorbers might also have advantages over the porous absorber as the honeycomb geometry has smaller heat loss due to re-radiation than foam disks which allows for better temperature distribution and therefore better performance [58]. Within ceramic materials, SiC might be better suited than Alumina due to its higher thermal conductivity. However, overall, these porous absorbers do experience large temperature fluctuations throughout the reforming process which can lead to material degradation. Other designs such as heat pipe reactors or tubular reactors with liquid beds lead to much smaller temperature variations but suffer in terms of methane conversion. Overall careful consideration must be paid to the heat transfer effects within the reactor whether it a porous solid, liquid bed, etc. as these effects can have great impact on not only performance but also long term reactor operational stability. In general, whatever the catalytic element/reaction site is, it needs to sustain high temperatures (without material degradation) and allow for as much solar penetration throughout the entire element as possible.

For a more quantitative comparison, a few reforming systems along with various performance metrics are summarized in Table 3. Note that not all the previously discussed systems are shown in Table 3 as only the systems where enough detail was given to obtain interesting metrics for comparison are included.

System Design	Reactor Volume (cm^3)	Temperature (°C)	Max Conversion (%)	Residence Time (s)	Conversion Rate/volume (% $s^{-1}cm^{-3}$)
CAESAR Project [52] - dry reforming, Rh/Alumina catalyst, tested with parabolic dish, ceramic disk absorber as catalytic element, CO_2:CH_4 = 1	16084.95	750 - 1100	66	3	0.00137
Kodama Study [49] - dry reforming, Ru/γ-Al_2O_3 catalyst, tested with Xe-arc lamp light, Ni-Cr-Al metal foam disk as catalytic element, CO_2:CH_4 = 1	7.07	730 - 1030	73	0.4	25.81
Kodama Study [62] - dry reforming, Ni/Alumina catalyst, tested with infrared furnace, 50-50 mixture of K_2CO_3/Na_2CO_3 with catalyst as catalytic element, CO_2:CH_4 = 1	136.19	950	70	6	0.0857
Levy Study [58] - dry reforming, Rh/Alumina catalyst, tested with solar furnace, cordierite honeycomb absorber as catalytic element, CO_2:CH_4 = 1.3	3848.45	700 - 900	67	.5	.0348
Steinfeld Study [82] - metal oxide reforming, ZnO catalyst, tested with solar furnace, ZnO + CH_4 sent into receiver as receiver is heated by solar, CH_4:ZnO = 5-25	1570.80	730 - 1030	50	3	0.0106

Table 3: Quantitative comparison of solar reforming systems

In addition to the metrics previously reported (methane conversion and residence time), Table 3 also includes the conversion rate/volume for each system. This metric is calculated by dividing the maximum methane conversion by the residence time and then dividing by the reactor volume. The

conversion rate/volume gives a better sense of the true performance of each reforming system because it also takes into account the scale of the experiment. A even better metric would be the product production rate/volume, however most previous work does not give enough detail about reformer outlet composition for proper calculation of this metric.

From Table 3 it can be seen that the previous studies utilize a wide range of residence times. This large range can possibly be attributed to the scale of the experiments and the range of reactor temperatures desired as, in addition to solar flux, the flow rate can greatly affect the reactor temperature due to the convective heat transfer. The last three systems in Table 3 have a conversion rate/volume on the same order of magnitude. However, the CAESAR project and metal foam disk study have vastly different conversion rate/volume. The very low conversion rate/volume in the CAESAR project can be attributed to the experimental procedure in that it was found that the catalyst was not dispersed evenly within the absorber as well as absorber material degradation during the reforming experiments. Both of these aspects can affect the reformer performance and contribute to the much lower conversion rate/volume calculated. Moreover, the CAESAR project was an early proof of concept study and thus, optimal performance was not necessarily the primary focus.

On the other end of the spectrum, the metal foam disk study has a conversion rate/volume that is significantly higher than any of the other reformer studies. The very high conversion rate/volume can possibly be attributed to the scale of the experiment as this study was done on a lab scale with a very small absorber. Another factor could be the use of a

metallic absorber as opposed to a ceramic absorber used in many of the other studies. This results suggests that, since the metallic absorber would presumably be more conductive than the ceramic absorber, having a more conductive catalytic element allows for a more even temperature distribution within the catalytic element which leads to higher conversion and better reformer performance.

5. Recent Developments

Based on what has been presented, two areas for potential innovation are membrane solar reformers and chemical looping solar reformers. These will now be discussed further, followed by a discussion of research needs.

5.1. Membrane-Based Solar Reformer

Membrane-based reformers have been proposed because they allow for significant methane conversion at relatively low temperatures ($< 600°C$) [84]. These reformers operate by using a hydrogen permeable membrane to remove hydrogen from the reaction zone which in turn shifts the equilibrium of the reforming reaction to allow for more methane conversion [85, 86]. While designs for traditional membrane-based reformers (i.e., no solar) have been proposed and experimentally studied [87, 88, 89], there has not been much experimental work on the subject of solar membrane-based reformers. Numerical studies have been done on pairing membrane-based reformers with molten salt streams heated by solar energy [78, 86]. The reformer design is similar to previously discussed tubular heat exchanger reformer concepts. In this study, steam reforming with a Pd membrane loaded with a MgO promoted Ni/Alumina catalyst is simulated [86]. Pd membranes are used

because of their permeable exclusivity to hydrogen [90, 91]. However, these Pd membranes have a high cost, but there have been recent work in mass production of Pd membranes at economically feasible costs [92].

Reaction zone temperatures of approximately 600-900 K were studied [86]. These temperatures were studied based on temperatures that can be achieved by parabolic trough solar collector systems. The simulation results show that significant increase in methane conversion can be achieved at relatively low temperatures through the use of these membrane reformers (Figure 32).

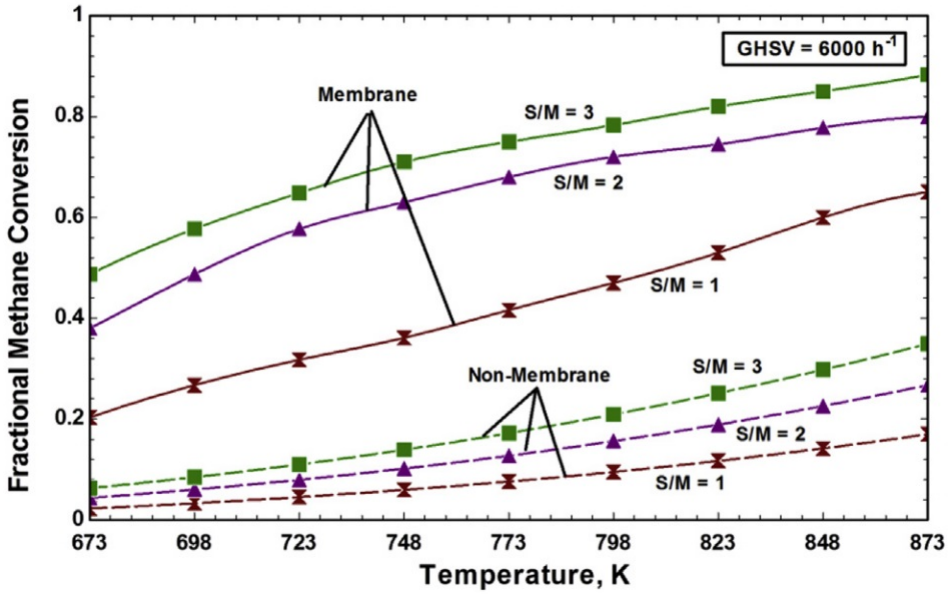

Figure 32: Methane conversion comparison for membrane and non-membrane reformer [86]

Moreover, the simulations showed that the reformer performance could be kinetically limited (due to the low activity of the Ni catalyst) or transport limited (due to hydrogen separation) depending on the operating conditions [86]. Therefore there is room for improvement in both catalyst and perme-

able membrane development that can allow for better performance in these low temperature reformers. Overall, these membrane-based solar reformers are able to achieve significant conversion at relatively low temperatures ($< 600°C$), and hence reduce the complexity and cost of the solar collector/concentrator.

Besides hydrogen permeable membranes, higher temperature oxygen permeable membranes offer another reforming opportunity. For these higher temperature settings, membrane reactors have been studied for use in water splitting [9, 93]. In this case, a mixed oxygen-ion-electron conducting ceramic membrane is used in the temperature range of 700-900°C [9]. These membranes, when exposed to a oxygen partial pressure gradient, are oxygen selective-permeable. As the oxygen in ionic form is transported across the membrane (due to the pressure gradient), there is a simultaneous flux of electrons in the opposite direction to charge compensate for the oxygen flux. These membranes have either a fluorite or perovskite crystal structure [94]. Common fluorite based membranes include bismuth oxide and zirconia based materials, and common perovskite based membranes include LCF, BCFN, and LSCF [94, 95].

A schematic of this type of membrane reactor is shown in Figure 33. The oxygen ions are transported across the membrane towards the reducing side leaving hydrogen on the oxidizing side. The oxygen on the reducing side can be used to partially oxidize methane, which, by reducing the oxygen partial pressure on this side, contributes to raising the oxygen flux and hence the rate of water splitting and hydrogen production on the oxidizing side. Oxygen flux enhancement and its impact on hydrogen production by water splitting

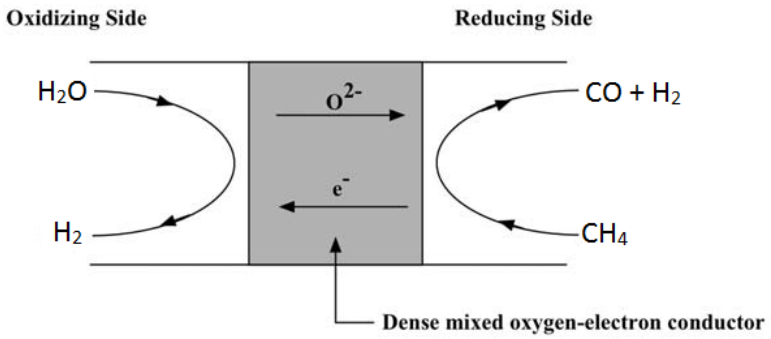

Figure 33: Schematic of water splitting and methane reforming membrane reactor (adapted from [9])

was demonstrated in [93]. From experimental studies it was discovered that the oxygen flux increased by more than 50 times when using a reactive gas on the reducing side (as compared to using an inert) which leads to an increase in hydrogen production [93]. Moreover, in these reactors, the performance is kinetically limited by the surface reactions on the membrane [93]. Thus, further improvements can potentially be made by using a catalyst on the membrane [96]. In terms of integrating the membrane reactor with the solar collectors, the membrane system would be directly heated with reforming reactions occurring on one side of the membrane (most likely the side being heated).

5.2. Chemical Looping Solar Reformer

Another reforming concept that has been suggested utilizes metal redox reforming in the solar reforming context [10]. In this process a metal oxide is used to partially oxidize/reform methane followed by the subsequent oxidation of the metal with water in a water splitting reaction (see Section 3.5). Previous work has explored the implementation of this process utiliz-

ing a switching operation [10]. In other words, input into the reformer is switched periodically between fuel and steam. This may not always be desirable as it results in varying output (switching between syngas and pure hydrogen) which might not be suited for integration with the rest of the plant, e.g., a power cycle. Moreover, there are operational complexities associated with continuously switching inlet streams that may be difficult to implement. An alternative is to use two separate fluidized bed reactors, one for the reduction step and one for the oxidation step. This fluidized bed chemical looping reactor system has been proposed before for oxy-combustion and steam/autothermal reforming systems [97].

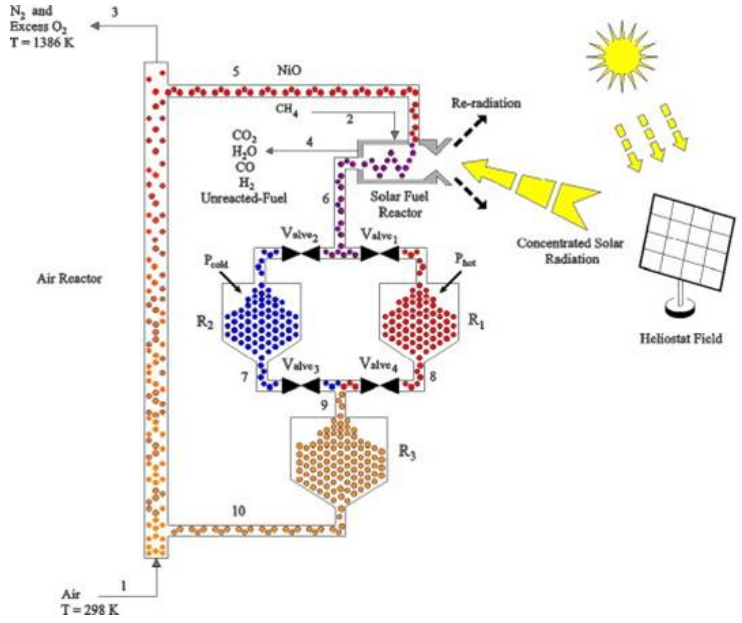

Figure 34: Schematic of solar CLC system with solar energy storage [98]

In the solar context, a fluidized bed chemical looping combustion system has been proposed to replace the traditional combustor in a solarized gas

turbine system [99, 100], with the solar energy used to heat the fuel reactor (reduction reactor). In these systems, the solar energy is utilized at a temperature between 500°C and 600°C [99, 100]. Because for the partial oxidation of methane (an exothermic reaction) only moderate temperatures are needed from the solar collector. Another study has also investigated the use of a solar chemical looping system that allows for the storage of solar energy within the oxygen carrier (metal oxide) particles [98]. A schematic of the system is shown in Figure 34. This system has additional reservoirs to store the oxygen carrier particles. While this proposed system utilized air as the oxidizing stream, steam or CO_2 could be used instead [80, 81]. Using steam or CO_2 results in the indirect steam/dry reforming process discussed previously in Section 3.5. Also, as discussed previously, a number of different oxygen carriers can be used besides the NiO proposed in [98]. Other oxygen carriers than could potentially be used include Cu, Fe, W, and Zn with W shown to be the most reactive [10, 80].

While fluidized bed chemical looping reformers eliminate the need for periodic operation, they may suffer from large pressure drops and operational complexity. An alternative reactor design that enables continuous operation with lower pressure drop is the rotary reactor [101]. In this reactor, a wheel rotates between different input zones (steam and fuel). The oxygen carrier is coated on to the honeycomb surface of the reactor wheel. This concept has been applied to oxy-combustion (Figure 35) [101, 102, 103, 104]. The same reactor design (Figure 35) has also been proposed for chemical looping water splitting with Pr-CeO_2 as the oxygen carrier [105]. Experimental results have shown that total hydrogen production can be 10-40 times the amount

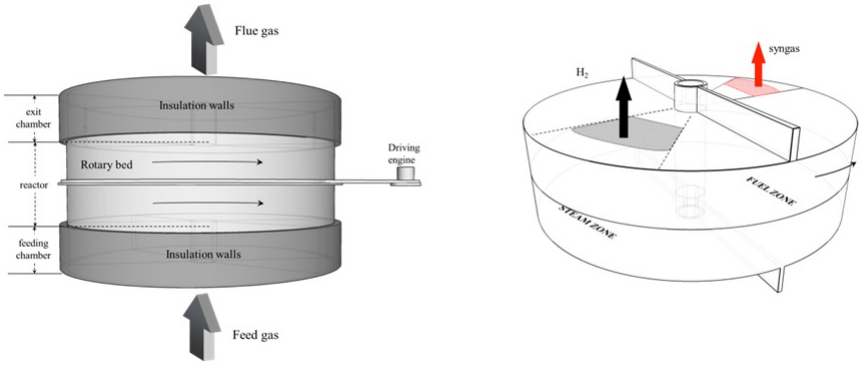

Figure 35: Schematic of rotary reactor for oxy-combustion [101]

produced by thermochemical cycles [105]. Moreover, the syngas produced has a CO/H_2 ratio close to 1:2 (ideal for other industrial processes), and there was minor carbon deposition [105].

A slightly different rotary reactor has also been proposed for solar hydrogen production through a two step water splitting process [106]. A schematic of this reactor is shown in Figure 36. The cylindrical rotor was coated with reactive ceramics (metal oxide) and as the rotor rotated through being heated by the solar energy, the metal oxide was reduced (endothermic process) and released oxygen. While the rotor was not being heated by the solar energy, the reduced metal oxide would split the water to produce hydrogen. The thermal energy required for the water splitting reaction was obtained from the the solar energy absorbed during the reduction process. In this reactor, CeO_2 and Ni,Mn-ferrite were used as the reactive ceramics with hydrogen production observed at a reactor temperature of 1273 K and 1173 K, respectively [106].

A chemical looping reformer allows for more flexibility in design as a

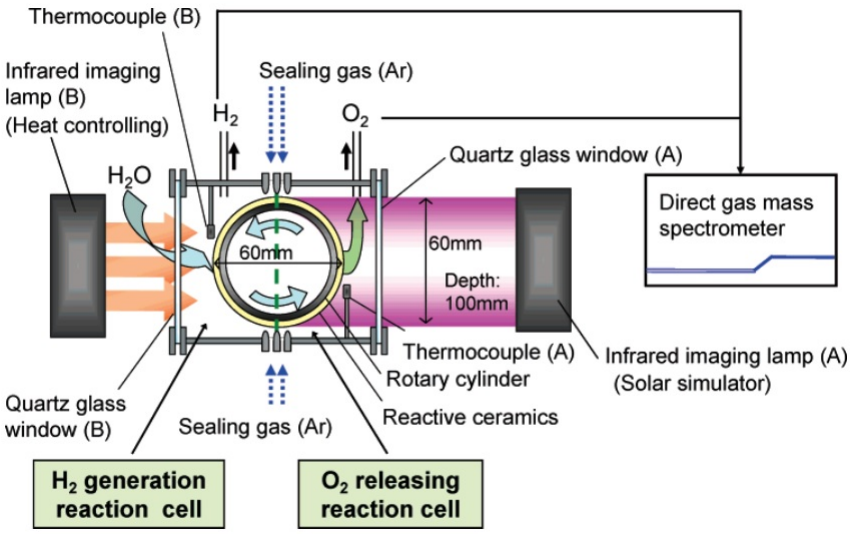

Figure 36: Schematic of solar rotary reactor for water splitting [106]

number of different metal oxides can be used (discussed previously in Section 3.5). Moreover, a noble metal catalyst is not necessary. Furthermore, the steam redox process used in chemical looping can produce a product with a lower H_2/CO ratio than the traditional direct steam reforming process which is more desirable for other industrial processes. Steam redox also produces a pure hydrogen stream which can be useful in a number of different applications.

5.3. Research Needs

Much of the previous work has been experimental. Moreover, while there has been some commercial scale experimental work (CAESAR, ASTERIX, SOLASYS, and SOLREF projects), most of the experimental work has been on the lab scale. There is a need for computational models that allow for further, more in-depth analysis of these types of reforming systems. In or-

der to develop a reasonably high fidelity model, various processes need to be accounted for including the kinetics of the reforming reactions and the heat transfer between the environment and the reaction site as well as within the reaction site itself at typical high operating temperatures. The reaction kinetics may require additional experimental work in order to obtain a suitable mathematical representation for them as most of the current kinetic studies are extrinsic and therefore are highly dependent on the specific experimental setup. Intrinsic kinetic studies would allow for the application of kinetic parameters to a wide range of reformer designs.

Development of computational models allow for more detailed study of heat transfer effects including how material properties (i.e., heat capacity, conductivity, emissivity, etc.) or reactor design (size, flow rate, concentration of solar flux etc.) can affect the absorption of the solar radiation and temperature distribution within the reactor. The understanding of how solar radiation is absorbed within the reactor can in turn help determine which aspects of the reactor design are most important in achieving a more even temperature distribution which is beneficial for long term reactor operation. Furthermore, previous work with porous absorber reformers has shown that most of the heat transfer occurs in the front half of the absorber which suggests that the solar energy is not necessarily utilized within the entirety of the reactor. Therefore, computational models allow for the study of this balance between using the solar energy as efficiently as possible while also allowing for the reactor sizes to be large enough to achieve significant conversion. In addition, the computational model can be used to simulate scaled up versions of the lab scale experimental setups investigated previously which

would in turn allow for the determination of limiting factors for scaling as well as potential performance of a larger scale solar reforming system.

6. Conclusion

Overall, there has been much experimental work done on solar reforming systems. The solar reforming systems can be divided into three main categories based on reforming process: steam reforming, dry reforming ,and redox reforming systems. Within these categories there are directly and indirectly heated reformers. Directly heated reformers can reach higher operating temperatures which leads to higher fuel conversion and the reforming process is usually reaction rate limited. On the other hand, indirectly heated reformers, while not able to reach as high of an operating temperature, do not have the size limitations associated with directly heated reformers. For these solar reforming systems, the design of the reformer as well as how it is heated (i.e., directly heated porous absorber, heated tubular reactor, liquid bed, etc.) can affect a number of different aspects of reformer performance including not only the methane conversion but also the temperature distribution/variation within the reformer which can in turn affect the reactor's long term operational stability. The directly heated porous absorbers were shown to achieve highest methane conversion but also larger temperature variations. The liquid bed reactors were shown to have very small temperature variations (due to the higher heat capacity of the liquid bed) but lower methane conversions. The catalyst used is also an important aspect to consider as with higher operating temperatures, the catalyst has a potential to degrade and become inactive and thus needs to be chosen accordingly. Noble

metal catalysts such as Rh or Ru have been shown to perform well at these higher temperatures, however, economic limitations may require the sacrifice of some performance with use of cheaper transition metal catalysts (like Ni). The use of noble metal catalysts could be eliminated through the use of membrane-based or chemical looping reformers. Membrane-based reformers can achieve high conversion at relatively low temperatures which eliminates the need for noble metal catalysts. In chemical looping reformers, the oxygen carrier acts as the "catalyst" and a number of different carriers can be used including Ni, Fe, and Cu. Computational models should also be developed in order to further study the balance between the heat transfer and chemical processes, which in turn allows for the optimization of reactor design with regards to maximizing conversion and utilizing the solar energy efficiently.

Acknowledgment

The authors would like to thank the King Fahd University of Petroleum and Minerals in Dhahran, Saudi Arabia, for funding the research reported in this article through the Center for Clean Water and Clean Energy at MIT and KFUPM under project number R12-CE-10.

References

[1] Kodama, T.. High-temperature solar chemistry for converting solar heat to chemical fuels. Progress in Energy and Combustion Science 2003;29(6):567 – 597.

[2] Steinfeld, A., Weimer, A.W.. Thermochemical production of fuels with concentrated solar energy. Optics Express 2010;18(S1):A100–A111.

[3] Zedtwitz, P., Petrasch, J., Trommer, D., Steinfeld, A.. Hydrogen production via the solar thermal decarbonization of fossil fuels. Solar Energy 2006;80(10):1333 – 1337.

[4] Fletcher, E.A.. Solar thermochemical and electrochemical research - how they can help reduce the carbon dioxide burden. Energy 1996;21(78):739 – 745.

[5] Ozalp, N., Kogan, A., Epstein, M.. Solar decomposition of fossil fuels as an option for sustainability. International Journal of Hydrogen Energy 2009;34(2):710 – 720.

[6] Pregger, T., Graf, D., Krewitt, W., Sattler, C., Roeb, M., Möller, S.. Prospects of solar thermal hydrogen production processes. International Journal of Hydrogen Energy 2009;34(10):4256 – 4267.

[7] Steinfeld, A.. Solar thermochemical production of hydrogena review. Solar Energy 2005;78(5):603 – 615.

[8] Agrafiotis, C.C., Pagkoura, C., Lorentzou, S., Kostoglou, M., Konstandopoulos, A.G.. Hydrogen production in solar reactors. Catalysis Today 2007;127(14):265 – 277.

[9] Balachandran, U., Lee, T., Wang, S., Dorris, S.. Use of mixed conducting membranes to produce hydrogen by water dissociation. International Journal of Hydrogen Energy 2004;29(3):291 – 296.

[10] Kodama, T., Ohtake, H., Matsumoto, S., Aoki, A., Shimizu, T., Kitayama, Y.. Thermochemical methane reforming using a reactive WO_3/W redox system. Energy 2000;25(5):411 – 425.

[11] Muhich, C.L., Evanko, B.W., Weston, K.C., Lichty, P., Liang, X., Martinek, J., et al. Efficient generation of h2 by splitting water with an isothermal redox cycle. Science 2013;341(6145):540–542.

[12] Scheffe, J.R., McDaniel, A.H., Allendorf, M.D., Weimer, A.W.. Kinetics and mechanism of solar-thermochemical h2 production by oxidation of a cobalt ferrite-zirconia composite. Energy Environ Sci 2013;6:963–973.

[13] Wang, L., Murata, K., Inaba, M.. Production of pure hydrogen and more valuable hydrocarbons from ethane on a novel highly active catalyst system with a pd-based membrane reactor. Catalysis Today 2003;82(1-4):99 – 104.

[14] Epstein, M.. Solar thermal reforming of methane. Tech. Rep.; The Weizmann Institute of Science; 2010.

[15] Steinfeld, A., Meier, A.. Solar fuels and materials. In: in Chief: Cutler J. Cleveland, E., editor. Encyclopedia of Energy. New York: Elsevier; 2004, p. 623 – 637.

[16] Tamme, R., Buck, R., Epstein, M., Fisher, U., Sugarmen, C.. Solar upgrading of fuels for generation of electricity. Journal of Solar Energy Engineering 2001;123(2):160–163.

[17] Liu, J.A.. Kinetics, catalysis and mechanism of methane steam reforming. Masters Thesis, Worcester Polytechnic Institute; 2006.

[18] Stein, W., Edwards, J., Hinkley, J., Sattler, C.. Fuels hydrogen production — natural gas: Solar-thermal steam reforming. In: in Chief:Jrgen Garche, E., editor. Encyclopedia of Electrochemical Power Sources. Amsterdam: Elsevier; 2009, p. 300 – 312.

[19] Wagar, W., Zamfirescu, C., Dincer, I.. Thermodynamic analysis of solar energy use for reforming fuels to hydrogen. International Journal of Hydrogen Energy 2011;36(12):7002 – 7011.

[20] Möller, S., Kaucic, D., Sattler, C.. Hydrogen production by solar reforming of natural gas: A cost study. ASME Conference Proceedings 2004;2004(37475):505–514.

[21] Möller, S., Kaucic, D., Sattler, C.. Hydrogen production by solar reforming of natural gas: A comparison study of two possible process configurations. Journal of Solar Energy Engineering 2006;128(1):16–23.

[22] Agrafiotis, C., von Storch, H., Roeb, M., Sattler, C.. Solar thermal reforming of methane feedstocks for hydrogen and syngas production-a

review. Renewable and Sustainable Energy Reviews 2014;29(0):656 – 682.

[23] Romero, M., Steinfeld, A.. Concentrating solar thermal power and thermochemical fuels. Energy Environ Sci 2012;5:9234–9245.

[24] Simakov, D.S.A., Wright, M.M., Ahmed, S., Mokheimer, E.M.A., Roman-Leshkov, Y.. Solar thermal catalytic reforming of natural gas: a review on chemistry, catalysis and system design. Catal Sci Technol 2015;5:1991–2016.

[25] Ross, J.R.H.. Heterogeneous Catalysis Fundamentals and Applications. Elsevier; 2012.

[26] Angeli, S.D., Monteleone, G., Giaconia, A., Lemonidou, A.A.. State-of-the-art catalysts for {CH4} steam reforming at low temperature. International Journal of Hydrogen Energy 2014;39(5):1979 – 1997.

[27] Ashcroft, A.T., K., A., Cheetham, , Green, M.L.H., Vernon, P.D.F.. Partial oxidation of methane to synthesis gas using carbon dioxide. Nature 1991;(6332):225226.

[28] Rostrupnielsen, J., Hansen, J.. Co2-reforming of methane over transition metals. Journal of Catalysis 1993;144(1):38 – 49.

[29] Simakov, D.S., Luo, H.Y., Romn-Leshkov, Y.. Ultra-low loading ru/-al2o3: A highly active and stable catalyst for low temperature solar thermal reforming of methane. Applied Catalysis B: Environmental 2015;168-169(0):540 – 549.

[30] Tsang, S., Claridge, J., Green, M.. Recent advances in the conversion of methane to synthesis gas. Catalysis Today 1995;23(1):3 – 15.

[31] Claridge, J.B., York, A.P., Brungs, A.J., Marquez-Alvarez, C., Sloan, J., Tsang, S.C., et al. New catalysts for the conversion of methane to synthesis gas: Molybdenum and tungsten carbide. Journal of Catalysis 1998;180(1):85 – 100.

[32] Iyer, M.V., Norcio, L.P., Punnoose, A., Kugler, E.L., Seehra, M.S., Dadyburjor, D.B.. Catalysis for synthesis gas formation from reforming of methane. Topics in Catalysis 2004;29(3-4):197–200.

[33] Wu, H., La Parola, V., Pantaleo, G., Puleo, F., Venezia, A.M., Liotta, L.F.. Ni-based catalysts for low temperature methane steam reforming: Recent results on ni-au and comparison with other bi-metallic systems. Catalysts 2013;3(2):563–583.

[34] Liu, C.j., Ye, J., Jiang, J., Pan, Y.. Progresses in the preparation of coke resistant ni-based catalyst for steam and co2 reforming of methane. ChemCatChem 2011;3(3):529–541.

[35] Rostrup-Nielsen, J.R.. New aspects of syngas production and use. Catalysis Today 2000;63(2-4):159 – 164.

[36] Qin, D., Lapszewicz, J.. Study of mixed steam and {CO2} reforming of {CH4} to syngas on mgo-supported metals. Catalysis Today 1994;21(2-3):551 – 560.

[37] Rostrup-Nielsen, J.R.. Activity of nickel catalysts for steam reforming of hydrocarbons. Journal of Catalysis 1973;31(2):173 – 199.

[38] Wei, J., Iglesia, E.. Isotopic and kinetic assessment of the mechanism of methane reforming and decomposition reactions on supported iridium catalysts. Phys Chem Chem Phys 2004;6:3754–3759.

[39] Wei, J., Iglesia, E.. Isotopic and kinetic assessment of the mechanism of reactions of {CH4} with {CO2} or {H2O} to form synthesis gas and carbon on nickel catalysts. Journal of Catalysis 2004;224(2):370 – 383.

[40] Claridge, J.B., Green, M.L.H., Tsang, S., York, A.P.E., Ashcroft, A.T., Battle, P.D.. A study of carbon deposition on catalysts during the partial oxidation of methane to synthesis gas. Catalysis Letters 1993;22(4):299–305.

[41] Cobalt prices and cobalt price charts. http://www.infomine.com/investment/metal-prices/cobalt/; Accessed July 8, 2014.

[42] Engelhard Industrial Bullion (EIB) Prices. http://apps.catalysts.basf.com/apps/eibprices/mp/defaultmain.aspx; Accessed June 27, 2014.

[43] Yamaguchi, D., Tang, L., Burke, N., Chiang, K., Rye, L., Hadley, T., et al. Hydrogen Energy: Challenges and Perspectives; chap. 2. Intech; 2012, p. 31–54.

[44] Wang, S., Lu, G.Q.M., Millar, G.J.. Carbon dioxide reforming of methane to produce synthesis gas over metal-supported catalysts: state of the art. Energy & Fuels 1996;10(4):896–904.

[45] Maestri, M., Vlachos, D.G., Beretta, A., Groppi, G., Tronconi, E.. Steam and dry reforming of methane on rh: Microkinetic analysis and hierarchy of kinetic models. Journal of Catalysis 2008;259(2):211 – 222.

[46] Dahl, J.K., Weimer, A.W., Lewandowski, A., Bingham, C., Bruetsch, F., Steinfeld, A.. Dry reforming of methane using a solar-thermal aerosol flow reactor. Industrial & Engineering Chemistry Research 2004;43(18):5489–5495.

[47] Klein, H.H., Karni, J., Rubin, R.. Dry methane reforming without a metal catalyst in a directly irradiated solar particle reactor. Journal of Solar Energy Engineering 2009;131(2):021001–1–14.

[48] Kodama, T., Kondoh, Y., Kiyama, A., Shimizu, K.I.. Hydrogen production by solar thermochemical water-splitting/methane-reforming process. ASME Conference Proceedings 2003;2003(36762):121–128.

[49] Kodama, T., Kiyama, A., Shimizu, K.I.. Catalytically activated metal foam absorber for light-to-chemical energy conversion via solar reforming of methane. Energy & Fuels 2003;17(1):13–17.

[50] Kodama, T., Kiyama, A., Moriyama, T., Mizuno, O.. Solar methane reforming using a new type of catalytically-activated metallic foam absorber. Journal of Solar Energy Engineering 2004;126(2):808–811.

[51] Sang, L., Sun, B., Tan, H., Du, C., Wu, Y., Ma, C.. Catalytic reforming of methane with CO_2 over metal foam based monolithic catalysts. International Journal of Hydrogen Energy 2012;37(17):13037 – 13043.

[52] Buck, R., Muir, J.F., Hogan, R.E.. Carbon dioxide reforming of methane in a solar volumetric receiver/reactor: the CAESAR project. Solar Energy Materials 1991;24(14):449 – 463.

[53] Skocypec, R.D., Hogan Jr., R.E., Muir, J.F.. Solar reforming of methane in a direct absorption catalytic reactor on a parabolic dish: II-modeling and analysis. Solar Energy 1994;52(6):479 – 490.

[54] NIST property data summaries - sintered alumina. http://www.ceramics.nist.gov/srd/summary/ scdaos.htm; Accessed November 27, 2012.

[55] Muir, J.F., Jr., R.E.H., Skocypec, R.D., Buck, R.. Solar reforming of methane in a direct absorption catalytic reactor on a parabolic dish: I-test and analysis. Solar Energy 1994;52(6):467 – 477.

[56] Twigg, M.V., editor. Catalyst Handbook. Wolfe Publishing Ltd.; 1989.

[57] Berman, A., Karn, R.K., Epstein, M.. Steam reforming of methane on a Ru/Al_2O_3 catalyst promoted with mn oxides for solar hydrogen production. Green Chem 2007;9:626–631.

[58] Levy, M., Rubin, R., Rosin, H., Levitan, R.. Methane reforming by direct solar irradiation of the catalyst. Energy 1992;17(8):749 – 756.

[59] Anikeev, V., Bobrin, A., Ortner, J., Schmidt, S., Funken, K.H., Kuzin, N.. Catalytic thermochemical reactor/receiver for solar reforming of natural gas: Design and performance. Solar Energy 1998;63(2):97 – 104.

[60] High-flux solar furnace and xenon-high-flux solar simulator. http://www.dlr.de/sf/en/Portaldata/73/Resources/images/sonnenofen/Geometrie_eng.JPG; Accessed November 27, 2012.

[61] Gokon, N., Oku, Y., Kaneko, H., Tamaura, Y.. Methane reforming with CO_2 in molten salt using FeO catalyst. Solar Energy 2002;72(3):243 – 250.

[62] Kodama, T., Koyanagi, T., Shimizu, T., Kitayama, Y.. CO_2 reforming of methane in a molten carbonate salt bath for use in solar thermochemical processes. Energy & Fuels 2001;15(1):60–65.

[63] Diver, R., Fish, J., Levitan, R., Levy, M., Meirovitch, E., Rosin, H., et al. Solar test of an integrated sodium reflux heat pipe receiver/reactor for thermochemical energy transport. Solar Energy 1992;48(1):21 – 30.

[64] Spiewak, I., Tyner, C.E., Ulrich, . Applications of solar reformingtechnology. Tech. Rep.; Sandia National Laboratories; 1993.

[65] Segal, A., Epstein, M.. Solar ground reformer. Solar Energy 2003;75(6):479 – 490.

[66] Epstein, M., amd A. Segal, I.S., Levy, I., Lieberman, D., Meri, M., Lerner, V.. Solar experiments with a tubular reformer. In: Proceedings of the eighth international symposium on solar thermal concentrating technologies. Köln, Germany; 1996, p. 1209–29.

[67] Ben-Zvi, R., Karni, J.. Simulation of a volumetric solar reformer. Journal of Solar Energy Engineering 2007;129(2):197–204.

[68] Rubin, R., Karni, J., Yeheskel, J.. Chemical kinetics simulation of high temperature hydrocarbons reforming in a solar reactor. Journal of Solar Energy Engineering 2004;126(3):858–866.

[69] Rubin, R., Karni, J.. Carbon dioxide reforming of methane in directly irradiated solar reactor with porcupine absorber. Journal of Solar Energy Engineering 2011;133(2):021008–021008–5.

[70] Maria, G.D., Tiberio, C., D'Alessio, L., Piccirilli, M., Coffari, E., Paolucci, M.. Thermochemical conversion of solar energy by steam reforming of methane. Energy 1986;11(8):805 – 810.

[71] Maria, G.D., D'Alessio, L., Coffari, E., Paolucci, M., Tiberio, C.. Thermochemical storage of solar energy with high-temperature chemical reactions. Solar Energy 1985;35(5):409 – 416.

[72] Edwards, J.H., Duffy, G.J., Benito, R., Do, T., Dave, N., McNaughton, R., et al. CSIRO's solar thermal - fossil energy hybrid technology for advanced power generation. In: Proceedings of Solar Thermal 2000 10th SolarPACES International Symposium on Solar Thermal Concentrating Technologies. Sydney, N.S.W; 2000, p. 27–32.

[73] McNaughton, R., Hart, G., Collins, M.. Solar steam reforming using a closed cycle gaseous heat transfer loop. In: Proceedings of 2012 solarPACES, concentrating solar power and chemical energy systems conference. Marrakech, Morocco; 2012,.

[74] McNaughton, R., Stein, W.. Improving efficiency of power generation from solar thermal natural gas reforming. In: Proceedings of 15th in-

ternational solarPACES concentrating solar power symposium. Berlin, Germany; 2009,.

[75] Böhmer, M., Langnickel, U., Sanchez, M.. Solar steam reforming of methane. Solar Energy Materials 1991;24(14):441 – 448.

[76] Falco, M.D., Piemonte, V.. Solar enriched methane production by steam reforming process: Reactor design. International Journal of Hydrogen Energy 2011;36(13):7759 – 7762.

[77] Falco, M.D., Giaconia, A., Marrelli, L., Tarquini, P., Grena, R., Caputo, G.. Enriched methane production using solar energy: an assessment of plant performance. International Journal of Hydrogen Energy 2009;34(1):98 – 109.

[78] Giaconia, A., de Falco, M., Caputo, G., Grena, R., Tarquini, P., Marrelli, L.. Solar steam reforming of natural gas for hydrogen production using molten salt heat carriers. AIChE Journal 2008;54(7):1932–1944.

[79] Wörner, A., Tamme, R.. CO_2 reforming of methane in a solar driven volumetric receiver reactor. Catalysis Today 1998;46(23):165 – 174.

[80] Sheu, E.J., Ghoniem, A.F.. Redox reforming based, integrated solar-natural gas plants: Reforming and thermodynamic cycle efficiency. International Journal of Hydrogen Energy 2014;39(27):14817 – 14833.

[81] Sheu, E.J., Mokheimer, E.M., Ghoniem, A.F.. Dry redox reforming hybrid power cycle: Performance analysis and comparison

to steam redox reforming. International Journal of Hydrogen Energy 2015;40(7):2939 – 2949.

[82] Steinfeld, A., Brack, M., Meier, A., Weidenkaff, A., Wuillemin, D.. A solar chemical reactor for co-production of zinc and synthesis gas. Energy 1998;23(10):803 – 814.

[83] Steinfeld, A., Kuhn, P., Karni, J.. High-temperature solar thermochemistry: Production of iron and synthesis gas by Fe_3O_4-reduction with methane. Energy 1993;18(3):239 – 249.

[84] Gallucci, F., Fernandez, E., Corengia, P., van Sint Annaland, M.. Recent advances on membranes and membrane reactors for hydrogen production. Chemical Engineering Science 2013;92(0):40 – 66.

[85] Li, Y., Zhang, N., Cai, R.. Low co2-emissions hybrid solar combined-cycle power system with methane membrane reforming. Energy 2013;58(0):36 – 44.

[86] Said, S.A., Simakov, D.S., Mokheimer, E.M., Habib, M.A., Ahmed, S., Waseeuddin, M., et al. Computational fluid dynamics study of hydrogen generation by low temperature methane reforming in a membrane reactor. International Journal of Hydrogen Energy 2015;40(8):3158 – 3169.

[87] Simakov, D.S.A., Sheintuch, M.. Model-based optimization of hydrogen generation by methane steam reforming in autothermal packed-bed membrane reformer. AIChE Journal 2011;57(2):525–541.

[88] Simakov, D.S., Sheintuch, M.. Demonstration of a scaled-down autothermal membrane methane reformer for hydrogen generation. International Journal of Hydrogen Energy 2009;34(21):8866 – 8876.

[89] Patrascu, M., Sheintuch, M.. On-site pure hydrogen production by methane steam reforming in high flux membrane reactor: Experimental validation, model predictions and membrane inhibition. Chemical Engineering Journal 2015;262(0):862 – 874.

[90] Holleck, G.L.. Diffusion and solubility of hydrogen in palladium and palladium–silver alloys. The Journal of Physical Chemistry 1970;74(3):503–511.

[91] Yun, S., Oyama, S.T.. Correlations in palladium membranes for hydrogen separation: A review. Journal of Membrane Science 2011;375(12):28 – 45.

[92] Sheintuch, M., Simakov, D.. Alkanes dehydrogenation. In: De De Falco, M., Marrelli, L., Iaquaniello, G., editors. Membrane Reactors for Hydrogen Production Processes. Springer London; 2011, p. 183–200.

[93] Wu, X.Y., Chang, L., Uddi, M., Kirchen, P., Ghoniem, A.F.. Toward enhanced hydrogen generation from water using oxygen permeating lcf membranes. Phys Chem Chem Phys 2015;17:10093–10107.

[94] Sunarso, J., Baumann, S., Serra, J., Meulenberg, W., Liu, S., Lin, Y., et al. Mixed ionicelectronic conducting (miec) ceramic-

based membranes for oxygen separation. Journal of Membrane Science 2008;320(12):13 – 41.

[95] Yang, W., Wang, H., Zhu, X., Lin, L.. Development and application of oxygen permeable membrane in selective oxidation of light alkanes. Topics in Catalysis 2005;35(1-2):155–167.

[96] Dong, X., Jin, W., Xu, N., Li, K.. Dense ceramic catalytic membranes and membrane reactors for energy and environmental applications. Chem Commun 2011;47:10886–10902.

[97] Adanez, J., Abad, A., Garcia-Labiano, F., Gayan, P., de Diego, L.F.. Progress in chemical-looping combustion and reforming technologies. Progress in Energy and Combustion Science 2012;38(2):215 – 282.

[98] Jafarian, M., Arjomandi, M., Nathan, G.J.. A hybrid solar and chemical looping combustion system for solar thermal energy storage. Applied Energy 2013;103(0):671 – 678.

[99] Hong, H., Jin, H.. A novel solar thermal cycle with chemical looping combustion. International Journal of Green Energy 2005;2(4):397–407.

[100] Hong, H., Jin, H., Liu, B.. A novel solar-hybrid gas turbine combined cycle with inherent co[sub 2] separation using chemical-looping combustion by solar heat source. Journal of Solar Energy Engineering 2006;128(3):275–284.

[101] Zhao, Z., Chen, T., Ghoniem, A.F.. Rotary bed reactor for chemical-looping combustion with carbon capture. part 1: Reactor design and model development. Energy & Fuels 2013;27(1):327–343.

[102] Zhao, Z., Chen, T., Ghoniem, A.F.. Rotary bed reactor for chemical-looping combustion with carbon capture. part 2: Base case and sensitivity analysis. Energy & Fuels 2013;27(1):344–359.

[103] Zhao, Z., Iloeje, C.O., Chen, T., Ghoniem, A.F.. Design of a rotary reactor for chemical-looping combustion. part 1: Fundamentals and design methodology. Fuel 2014;121:327 – 343.

[104] Zhao, Z., Ghoniem, A.F.. Design of a rotary reactor for chemical-looping combustion. part 2: Comparison of copper-, nickel-, and iron-based oxygen carriers. Fuel 2014;121:344 – 360.

[105] Zhao, Z., Uddi, M., Tsvetkov, N., Yildiz, B., Ghoniem, A.. Redox study of fuel reduced ceria for chemical looping water splitting. In Preparation 2015;.

[106] Kaneko, H., Miura, T., Fuse, A., Ishihara, H., Taku, S., Fukuzumi, H., et al. Rotary-type solar reactor for solar hydrogen production with two-step water splitting process. Energy & Fuels 2007;21(4):2287–2293.